

Histoarchitecture of the liver and spleen in the interspecific hybrids of common carp (*Cyprinus carpio*) and gibel carp (*Carassius gibelio*)

Authors: Valigurová, Andrea, Hodová, Iveta, Vetešník, Lukáš, and Šimková, Andrea

Source: Journal of Vertebrate Biology, 74(24098)

Published By: Institute of Vertebrate Biology, Czech Academy of Sciences

URL: <https://doi.org/10.25225/jvb.24098>





The BioOne Digital Library (<https://bioone.org/>) provides worldwide distribution for more than 580 journals and eBooks from BioOne's community of over 150 nonprofit societies, research institutions, and university presses in the biological, ecological, and environmental sciences. The BioOne Digital Library encompasses the flagship aggregation BioOne Complete (<https://bioone.org/subscribe>), the BioOne Complete Archive (<https://bioone.org/archive>), and the BioOne eBooks program offerings ESA eBook Collection (<https://bioone.org/esa-ebooks>) and CSIRO Publishing BioSelect Collection (<https://bioone.org/csiro-ebooks>).

Your use of this PDF, the BioOne Digital Library, and all posted and associated content indicates your acceptance of BioOne's Terms of Use, available at www.bioone.org/terms-of-use.

Usage of BioOne Digital Library content is strictly limited to personal, educational, and non-commercial use. Commercial inquiries or rights and permissions requests should be directed to the individual publisher as copyright holder.

BioOne is an innovative nonprofit that sees sustainable scholarly publishing as an inherently collaborative enterprise connecting authors, nonprofit publishers, academic institutions, research libraries, and research funders in the common goal of maximizing access to critical research.

Histoarchitecture of the liver and spleen in the interspecific hybrids of common carp (*Cyprinus carpio*) and gibel carp (*Carassius gibelio*)

Andrea VALIGUROVÁ^{1*} , Iveta HODOVÁ¹ , Lukáš VETEŠNÍK^{1,2}  and Andrea ŠIMKOVÁ¹ 

¹ Department of Botany and Zoology, Faculty of Science, Masaryk University, Brno, Czech Republic; e-mail: andreav@sci.muni.cz, hodova@sci.muni.cz, simkova@sci.muni.cz

² Institute of Vertebrate Biology, Czech Academy of Sciences, Brno, Czech Republic; e-mail: vetesnik@ivb.cz

► Received 18 September 2024; Accepted 25 November 2024; Published online 28 January 2025

Abstract. Hybridisation is a commonly reported phenomenon in fish. This study focuses on cyprinid species, *Cyprinus carpio* and *Carassius gibelio* and their hybrids, including F1, F2 and backcross generations obtained by artificial breeding, to investigate the effect of the various types of crossbreeding representing different genomic contributions of common carp and gibel carp on the health and histoarchitecture of key organs involved in metabolism and immunity – the liver and spleen. Comparative histology revealed no clear trend in the organisation of liver and spleen parenchyma based on the type of crossbreeding. However, there are similarities between certain fish lines, most noticeable in the specific properties of hepatocytes and the pattern of glycogen distribution in their cytoplasm, and in the organisation of splenic fibrous skeleton. Moreover, this study suggests that long-term breeding of wild fish species in artificial conditions can affect their physiology, as we noted extravascular haemolysis affecting parts of the splenic parenchyma and small foci of hepatic necrosis. Compared to gibel carp and hybrid lines, the common carp with a longer history of cultivation showed the mildest forms of the pathologies detected, indicating that it coped best with the conditions of artificial breeding.

Key words: cyprinid fish, hybridisation, hepatic and splenic parenchyma, glycogen, histology

Introduction

Common carp *Cyprinus carpio* Linnaeus, 1758 and gibel carp *Carassius gibelio* Bloch, 1782 are phylogenetically closely related freshwater fishes commonly found in Czech aquaculture. While common carp is a commercially important fish, gibel carp is an invasive fish entering breeding ponds, whose expansion into new territories is mainly attributed to its reproductive strategy combining sexual and gynogenetic reproduction, i.e. asexual reproduction in which offspring are formed

parthenogenetically, but the egg development is induced by sperm of the same or phylogenetically closely related sexually reproducing species (Fuad et al. 2021). The gibel carp was imported to Europe from Chinese aquaculture around 1611-1691. Repeated introductions and translocations (including public releases) resulted in an extremely wide distribution of gibel carp across Europe, with its later invasions into all suitable aquatic environments (Copp et al. 2005). Following the invasion of gibel carp into breeding ponds for common carp, combined morphological and molecular diagnostics revealed

* Corresponding Author

This is an open access article under the terms of the Creative Commons Attribution Licence (CC BY 4.0), which permits use, distribution and reproduction in any medium provided the original work is properly cited.



the occurrence of F1 hybrids of these two fish species (Šimková et al. 2015).

Hybrid genotypes may possess lower, equivalent or higher levels of fitness relative to their parental taxa (Arnold & Hodges 1995, Burke & Arnold 2001). Usually, F1 hybrids are superior to their parents in traits related to the development, growth and resistance to environmental factors and show higher fitness and survival (e.g. Sun et al. 2016, Bartley et al. 2000, Šimková et al. 2021). In contrast, the hybrids of post-F1 generations often show reduced fitness as they suffer from sterility, low survival, developmental abnormalities and high susceptibility to pathogens (Renaut et al. 2009, Renaut & Bernatchez 2011, Tichopád et al. 2020). The unidirectional hybridisation of common carp and gibel carp studied in Czech breeding ponds has been shown to result solely in the presence of F1 hybrids with *C. gibelio* mtDNA, which exhibit many fish health- and fitness-related traits intermediate between those of parental species (Šimková et al. 2013, 2015). While F1 hybrids usually exhibit heterosis advantage for fitness-related traits (including the resistance to parasites) and are characterised by high vigour, the post-F1 generations of fish hybrids (backcrosses and F2 generations) often exhibit low viability and reduced survival due to asymmetrical genetic incompatibilities (i.e. hybrid breakdown; Stelkens et al. 2015, Šimková et al. 2022). The body shape morphology of F1 hybrids (common carp × gibel carp) is intermediate between parental species (Šimková et al. 2015). Based on the intermediate values of intestine size as well as cholesterol and glucose concentrations, their study suggests that hybridisation determines the food range, nutritional status, metabolic activity, and energy intake in hybrid offspring.

Previous research on F1 and post-F1 hybrids of common carp and gibel carp emphasised the need to investigate the effects of various types of crossbreeding representing different genomic contributions of common carp and gibel carp to the hybrid offspring on the vigour and immunocompetence of hybrids (Šimková et al. 2013, 2024, Vetešník et al. 2024). In this work, we focus on two organs, the liver and spleen, which play a key role in fish metabolism and immunity (Sales et al. 2017). The liver in fish represents an important metabolic centre that performs numerous vital functions, such as removing toxins, waste products and foreign particles from the bloodstream, regulating blood clotting and blood sugar levels, and producing essential nutrients (Berillis et al. 2011). It is crucial for metabolising nutrients absorbed in the

digestive tract and storing lipids, carbohydrates, iron and vitamin A. The liver covers the catabolism that breaks down metabolites to produce active energy (e.g. glycogenolysis, nitrogen) and the anabolism that uses these products (proteins, lipids, and carbohydrates) to build a new tissue needed for growth and reproduction. Due to its central role in fish physiology and immunity, the changes in hepatic tissue can serve as a good indicator of fish health (Berillis et al. 2011). The spleen is considered a major peripheral lymphoid organ in fish and is responsible for the induction of adaptive immune responses and has an important role in responses against pathogen invasion and elimination of immune complexes (Sales et al. 2017, Sayed et al. 2022, Zapata 2024). Moreover, it serves as a selective filter of the vascular system that performs hemocateresis and promotes lymphocyte maturation in cellular and humoral immunity (Press & Evensen 1999, Sales et al. 2017). In this study, we aimed to investigate the effect of the various types of crossbreeding representing different genomic contribution of *C. carpio* and *C. gibelio* on the health and architecture of the liver and spleen in their progeny lines obtained by artificial breeding. Since histology, despite the growing possibilities of applying molecular methods, still occupies an irreplaceable place in the evaluation of various pathological manifestations, we performed a comparative histological analysis of these two parenchymal organs in nine fish lines obtained by hybridisation between common carp and gibel carp (including F1, F2 and backcross generations).

Material and Methods

Fish collection and preparation of breed lines

The cyprinid species *C. carpio*, *C. gibelio*, and their naturally occurring F1 hybrids were caught from the Hlohovecký fishpond (48°46'51" N, 16°47'2" E; Danube River basin, Czech Republic) and transported live to the breeding facility. The identification and further handling of fish specimens and artificial breeding follow Šimková et al. (2022). The parental combinations listed in Table 1 were used for artificial spawning based on the mating of individual pairs (for the details, see Šimková et al. 2022). Nine fish lines resulting from artificial breeding were used for the study: i) single pure line of *C. carpio* (termed 'pure *C. carpio*' with the abbreviation 'CyCy'); ii) single pure line of *C. gibelio* (pure *C. gibelio*/CaCa); iii) two lines of the F1 generation: F1 with *C. gibelio* mtDNA (F1 *C. gibelio* × *C. carpio*/F1 CaCy) and F1 with *C. carpio* mtDNA (F1 *C. carpio* × *C. gibelio*/F1 CyCa); iv) four lines of backcrosses including two lines of maternal

Table 1. Summary of parental combinations used for artificial breeding and abbreviated designation of obtained fish lines. * Wild living F1 hybrids were offspring of *C. gibelio* female and *C. carpio* male.

Parents (species, gender)	<i>Cyprinus carpio</i> ♀	<i>Carassius gibelio</i> ♀	F1 hybrid ♀*
<i>Cyprinus carpio</i> ♂	CyCy	F1 CaCy	BC F1Cy
<i>Carassius gibelio</i> ♂	F1 CyCa	CaCa	BC F1Ca
F1 hybrid ♂*	BC CyF1	BC CaF1	F2

backcrosses (backcross *C. gibelio* × F1 hybrid/BC CaF1; backcross F1 hybrid × *C. gibelio*/BC F1Ca) and two lines of paternal backcrosses (backcross *C. carpio* × F1 hybrid/BC CyF1; backcross F1 hybrid × *C. carpio*/BC F1Cy); and v) single line of the F2 generation/F2 (both parents being representatives of the F1 generation with *C. gibelio* mtDNA). The fish were maintained under static conditions at 20 °C in aerated 90 L aquaria filled with settled tap water. The water in aquaria, with pH maintained at 7.2 ± 0.2 and conductivity ranging between 450–500 $\mu\text{S}/\text{cm}$, was filtered with an internal filter throughout the experiment. The fish were fed daily with frozen adult *Artemia*, dried pellets (www.exohobby.cz) and flakes (Tetra Min). All nine progeny lines were reared to the age of three years; the sample size and mean standard body length for each progeny line are provided in Table 2. The hepatopancreas and spleen were collected from all individuals by fish dissection and weighed to determine the values of the hepatosomatic (HSI) and spleen-somatic (SSI) indexes as follows: $\text{HSI} = (\text{hepatopancreas weight/body weight without viscera}) \times 100$; $\text{SSI} = (\text{spleen weight/body weight without viscera}) \times 100$. Control wild fish (*C. carpio*, *C. gibelio* and F1 hybrids) were collected from Hlohovecký fishpond in November 2021.

Fish manipulation was in accordance with Law No. 207/2004 of the collections of Laws of the Czech Republic on the protection, breeding, and use of experimental animals. The study was conducted under the experimental project approved by the Ministry of Education, Sports and Youth (MŠMT in Czech) under document n. 33,579/2019-2. The experiment was approved by the Animal Care and Use Committee of the Faculty of Science, Masaryk University in Brno (Czech Republic). All methods were carried out following ARRIVE guidelines.

Histological analysis

Liver and spleen collected from three randomly selected individuals per experimental fish line (27 individuals in total), as well as three wild control fish for each of common carp, gibel carp and F1 hybrid with *C. gibelio* mtDNA (nine individuals in total), were fixed in AFA (alcohol-formalin-acetic acid) fixative

and processed using standard histological methods (Valigurová & Koudela 2008). The tissues were embedded in BaWax (Bamed, Czech Republic) and sectioned to 7- μm thickness. Sections were stained with haematoxylin-eosin, Masson's trichrome (fast green method) or Alcian Blue-Periodic Acid-Schiff technique (Humason 1967). The Periodic Acid-Schiff (PAS) technique was used to visualise the glycogen in the liver. Its combination with Alcian Blue staining allowed to distinguish neutral and acid mucins, where Alcian blue at pH 2.5 stains acid mucins deep blue and subsequent application of the PAS stains the neutral mucins bright magenta, while tissues/cells containing both the acid and neutral mucins may show a dark blue or purple staining (Myers 2024). Stained and mounted sections were subjected to histological analysis using a motorised Olympus microscope BX61 with a digital camera and software. Tissue processing, specific staining and light microscopic observations were always performed under the same conditions and within one set simultaneously containing all specimens (i.e. all fish lines). Terminology used in this study follows previously published histopathological works (Wolf & Wolfe 2005, Wolf & Wheeler 2018, Torbenson et al. 2022).

Ultrastructural analysis

Liver tissue samples were fixed in 2.5% glutaraldehyde in 0.1 M cacodylate buffer, post-fixed with 1% OsO_4 in cacodylate buffer, dehydrated in the ethanol series and embedded into Epoxy resin blocks. The ultrathin sections were made using Reichert Ultracut E ultramicrotome and stained according to the standard protocol (Valigurová & Koudela 2008). Samples were observed with a JEOL-1010 transmission electron microscope. Tissue processing, staining and electron microscopic observations were performed under the same conditions and within one set simultaneously containing all specimens.

Results

Liver

Gross examination of the liver showed no definite shape of this organ in specimens of all fish lines.

Table 2. Summarisation of standard body lengths and sample sizes for experimental fish lines derived from artificial breeding.

Progeny line/Measurements	CyCy	CaCa	F1 CaCy	BC CaF1	BC F1Ca	BC CyF1	BC F1Cy	F2
Standard body length in mm (mean \pm SD)	141.9 \pm 14.3 (n = 8)	105.7 \pm 12.5 (n = 8)	131.1 \pm 17.1 (n = 8)	120.2 \pm 3.7 (n = 8)	121.4 \pm 11.1 (n = 8)	119.7 \pm 8.2 (n = 8)	134.1 \pm 10.4 (n = 8)	122.7 \pm 13.2 (n = 8)
								135.3 \pm 8.9 (n = 4)

Macroscopic differences in the livers among fish lines were observed mainly in the size, firmness and colour of the tissue. These differences were most pronounced in the pure lines of common carp and gibel carp: while the liver of common carp was brown and had the usual texture, the gibel carp liver was pale and appeared to be much more fluid, and it was larger than in common carp. All fish lines resulting from breeding with at least one parent being gibel carp had a more liquid liver. The hepatosomatic indexes (HSI, mean \pm SD) for all fish lines are provided in Table 3.

Histopathological analysis using three staining techniques, haematoxylin-eosin (HE), Masson's trichrome (MT) and Alcian Blue-Periodic Acid-Schiff (AB-PAS), supported by transmission electron microscopy (TEM), was used to assess differences in the general architecture of liver tissue and cytological characteristics of hepatocytes among all fish lines (Figs. 1-7). The serial sections of the liver of all fish lines showed the organisation of hepatocytes in a continuous cell mass interrupted by sinusoids, isolated vessels and bile ducts. No typical hexagonal lobules were observed (i.e. the lobules were absent from connective tissue septa), the parenchyma arrangement (i.e. the hepatocyte-sinusoidal structures) corresponded to the tubular form with double-layered hepatocyte lining separated by sinusoids. The predominantly polyhedral hepatocytes possessed a large spherical nucleus (mostly eccentrically located) with a prominent dark nucleolus. The AB-PAS reaction revealed differences in glycogen abundance and distribution in individual fish lines (Figs. 2, 4 and 6). No fish line showed signs of fatty degeneration (Figs. 1-7). Interestingly, the livers of all fish lines showed mild to severe sinusoidal congestion and dilated sinusoids with occasional hemosiderosis. Signs of cell death (e.g. shrinkage of hepatocytes, pyknosis or nuclear karyorrhexis, karyolysis, cell lysis, presence of cell debris and occasionally apoptotic bodies) as well as regeneration of liver parenchyma were present in all fish lines. Moreover, the liver parenchyma of both experimental and wild control fish showed more significant necrotic changes that were localised mainly on its periphery and in the range of spotted focal/multifocal to confluent necrosis. Necrotic foci were accompanied by mild or no inflammatory infiltration and fibrotic changes in some fish lines. Since these pathological manifestations showed no association with any fish line, they are not further described or included in the comparative histology, but the summary and evaluation of their range can be found in Table 3. The other histomorphological and

Table 3. Summary and ratings of specific characteristics observed during the histopathological evaluation of the liver and spleen in experimental fish lines.

Progeny line/Character	CyCy	CaCa	F1 CaCy	F1 CyCa	BC CaF1	BC F1Ca	BC CyF1	BC F1Cy	F2
Liver									
HSI (mean ± SD)	1.337 ± 0.429 (n = 6)	3.506 ± 0.781 (n = 6)	1.678 ± 0.237 (n = 6)	1.488 ± 0.161 (n = 5)	2.080 ± 0.416 (n = 6)	1.541 ± 0.381 (n = 6)	1.350 ± 0.236 (n = 7)	1.606 ± 0.383 (n = 6)	2.531 ± 1.051 (n = 3)
Presence of MMCs	3	1	2	2+	1	1	1+	2	1+
Hepatocyte hypertrophy	0	2	0	0	3	2+	1+	0	1
Distinctness of hepatocyte boundaries	1	3+	1+	3	3	3+	3	2	3
Hepatocellular vacuolisation	0	3	1	2+	3	3	3	2	3
Lipid deposition	3	0	1	1	1+	1	2	1+	1
Granularity of hepatocyte cytoplasm	3+	2	3	2	2+	2	2	2	1
Glycogen accumulation in hepatocytes	1	3	2+	3+	3+	3+	3	2	3
RER in hepatocytes	1	3	1+	3	2	3	2	2	3
Mitochondria in hepatocytes	3+	2	3+	3	2	1	3	3	2+
Mitochondrial swelling in hepatocytes	0	3	2	2	1	3+	2	1	1
Lysosomes in hepatocytes	2	1+	3	1+	1	1	2	2	2
Autophagosomes in hepatocytes	2	1+	1	2	3	1	1	3	3
Sinusoidal congestion	2	2	1	1+	3	2+	3	2	3
Spotty to multifocal necrosis	1	2	1+	1+	3	2	2	2	3+
Fibrosis	0	0	2	0	1	0	1+	0	1+
Inflammatory infiltration	2	1	1+	1	1	1	2	1	2
Spleen									

Table 3. Summary and ratings of specific characteristics observed during the histopathological evaluation of the liver and spleen in experimental fish lines.

Progeny line/Character	CyCy	CaCa	F1 CaCy	F1 CyCa	BC CaF1	BC F1Ca	BC CyF1	BC F1Cy	F2
SSI (mean ± SD)	0.235 ± 0.056 (n = 6)	0.200 ± 0.096 (n = 6)	0.186 ± 0.078 (n = 6)	0.231 ± 0.060 (n = 5)	0.314 ± 0.082 (n = 6)	0.328 ± 0.095 (n = 6)	0.281 ± 0.058 (n = 7)	0.248 ± 0.054 (n = 6)	0.228 ± 0.135 (n = 3)
Presence of MMCs	2	2	2	3	1	3	3+	3	3
Cell density in white pulp	1	3	1	1	1+	2+	1	1	2
Increased collagen deposition	0	1	1	0	1	1	0	1	1
Haemolysis	1	3	3+	3	2+	2+	2	3	2+
Enlarged erythrocytes	0	1+	1	0	1	1	1	2	0
Necrosis	0	1	1	1	0	0	0	1	2

0 – monitored character missing or not observed; 1 – low intensity or occurrence of monitored character; 2 – medium intensity or occurrence; 3 – high intensity or occurrence. The symbol + indicates a more pronounced increase in the intensity or frequency of the monitored character. Scored and averaged from all photomicrographs taken from histological, semithin and ultrathin sections of liver and spleen obtained from three individuals per fish line. Note: detailed information on fish lines and parental combinations used for artificial breeding can be found in Material and Methods (subchapter Fish collection and preparation of breed lines).

ultrastructural characteristics of the liver parenchyma are described below for each of the fish lines.

Pure *C. carpio* (CyCy): dark brown MMCs of small to medium sizes (up to 40 µm) were frequently seen scattered in the liver tissue. In liver parenchyma, the cell boundaries of hepatocytes were indistinct, and their shape was not regularly polyhedral (Figs. 1a and 2a). The cytoplasm of the hepatocytes was densely granulated with high affinity for plasma stains (eosin in HE and acid fuchsin/xylidine ponceau in MT), their spherical nuclei were regularly sized and contained a prominent central nucleolus (Fig. 1a). In HE-stained sections, both the nuclear lamina and nucleolus were stained purple, and the colouration of internal nuclear matrix was similar to the hepatocyte cytoplasm. Staining with MT confirmed confirmed confirmed the granular structure of the hepatocyte cytoplasm as well as the regular shape of the nucleus. Liver sections stained with AB-PAS showed a low glycogen load in the hepatocyte cytoplasm with a granular pattern (Fig. 2a). While histological sections showed no lipid deposition, semithin and ultrathin sections revealed lipid droplets of various sizes scattered throughout the liver parenchyma. These were almost colourless or blue in semithin sections (stained with toluidine blue). The number of lipid droplets in hepatocytes varied; while some hepatocytes were free of fat, others showed numerous lipid droplets. In addition, some regions of the liver parenchyma showed higher lipid deposition than others. The observation under TEM confirmed the homogeneous and very dense granulation of the hepatocyte cytoplasm and low amount of glycogen particles (Fig. 7a). Moreover, it revealed the presence of abundant large mitochondria and irregularly distributed lamellae of the rough endoplasmic reticulum (RER). While mitochondrial swelling was not observed, vacuoles, lysosomes and large autophagosomes were commonly found in hepatocyte cytoplasm (not shown). The plasma membrane delimiting the hepatocyte was hardly discernible (Fig. 7a).

Pure *C. gibelio* (CaCa): darkly pigmented MMCs of small sizes were rarely found in the liver tissue. The liver parenchyma consisted of hypertrophic, more or less polyhedral hepatocytes with wavy borders (Figs. 1b and 2b). In a major part of the liver, the hepatocyte cytoplasm in MT- and HE-stained sections was almost colourless with few granules. Compared to CyCy, their irregularly shaped nuclei and nucleoli were smaller and condensed (Fig. 1b). The hepatocytes showed mild and uneven glycogen-type vacuolisation (Fig. 1b), and AB-PAS staining



revealed a high glycogen load in liver tissue (Fig. 2b). At lower magnification, PAS-stained hepatocytes in a major part of the parenchyma showed a brightly stained periphery and perinuclear space, while in the remaining part, intense staining gave the cells a cup-shaped appearance, leading to a plastic appearance of the tissue. Higher magnification revealed that the cytoplasm of the cup-shaped hepatocytes was packed with irregularly distributed glycogen of noticeably higher concentration. The second type of hepatocytes with a bright border showed glycogen accumulation at their periphery and in rays radiating from the nucleus. Neither histological, semithin, nor ultrathin sections demonstrated the presence of lipid droplets in the liver parenchyma. Fine structure analysis of hepatocytes showed their cytoplasm with low electron density being packed with abundant glycogen particles, mitochondria, and RER lamellae accumulating in the perinuclear space and beneath the plasma membrane (Fig. 7b). Differently sized clusters of dense granules were interspersed among glycogen particles of almost uniform size. The wavy appearance of the plasma membrane observed in the histological sections (Fig. 1b) was caused by the focal clustering of RER lamellae and mitochondria (Fig. 7b). Both the number of mitochondria and the amount of RER differed between individual hepatocytes in ultrathin sections and some hepatocytes additionally contained large lysosomes. A swelling of approximately half of the mitochondria was present in almost all hepatocytes. Autophagosomes were rare, lipid droplets were not observed in the cytoplasm of hepatocytes.

F1 *C. gibelio* × *C. carpio* (F1 CaCy): the darkly pigmented MMCs of small to medium sizes (up to 40 µm) were commonly observed in the liver tissue. In the organisation and structure of hepatocytes (i.e. hepatocytes with granular, strongly eosinophilic cytoplasm), the liver parenchyma resembled that of CyCy, but the hepatocyte nuclei showed more pronounced basophilic staining and carried irregularly shaped nucleolus (Figs. 1c and 2c). In addition, the hepatocytes had slightly more pronounced borders than seen in CyCy but these were not as distinct as in the other fish lines. In histological sections, only very mild and uneven glycogen-type vacuolisation of hepatocytes was observed, with some hepatocytes having more vacuolated cytoplasm than others (Fig. 1c). The AB-PAS staining revealed a moderate to high glycogen load with almost regular distribution throughout the liver tissue (Fig. 2c). The peripheral tissue stained less intensively with PAS than the central area and at higher magnification

the intense staining overlapped the hepatocyte boundaries. Although no lipid deposition was detected histologically, clusters of blue-stained lipid droplets were detected in some hepatocytes in semithin sections and were occasionally seen in ultrathin sections. Under TEM, the electron-dense cytoplasm of the hepatocytes was packed with abundant and large mitochondria and several RER lamellae (Fig. 7c). Although the plasma membrane was not underlined by the RER (seen in CaCa), the demarcation of the round hepatocytes by their plasma membrane was more pronounced than in CyCy. Also, the small cytoplasmic inclusions differed from those in CyCy in that they contained a higher amount of glycogen particles dispersed among dense granules (Fig. 7c). While hepatocytes contained numerous lysosomes, autophagosomes were only occasionally detected. A swelling of several mitochondria (of the many found in the cytoplasm) was conspicuous and found in almost every hepatocyte.

F1 *C. carpio* × *C. gibelio* (F1 CyCa): numerous small, darkly pigmented MMCs were scattered throughout the liver tissue (Fig. 3a). The liver parenchyma contained polyhedral hepatocytes that were clearly demarcated by their plasma membrane (Figs. 3a and 4a). In HE- and MT-stained sections, the hepatocyte cytoplasm showed significantly lower granularity and affinity for plasma dyes (Fig. 3a) when compared to CyCy and F1 CaCy lines. The hepatocyte nuclei of irregular shape and size showed an intensely stained matrix. Mild vacuolisation of hepatocyte cytoplasm visible in histological sections was of the glycogen type. The liver stained with AB-PAS showed abundant glycogen with almost regular distribution, where central tissue stained more intensively than the peripheral area (Fig. 4a), as observed in F1 CaCy. Due to a high glycogen load in the hepatocyte cytoplasm, it was impossible to observe the boundaries of individual cells in AB-PAS-stained sections. Ultrastructural analysis showed the hepatocyte cytoplasm of low density filled with abundant and homogeneously distributed glycogen particles and small clusters of electron-dense granules scattered between them (Fig. 7d). Abundant RER lamellae surrounding the mitochondria, glycogen particles and granular material completely filled the perinuclear space. Moreover, a thick irregular layer of RER underlined the hepatocyte plasma membrane (Fig. 7d), resulting in the distinct cell demarcation observed in histological sections (Fig. 3a). RER lamellae surrounded most of the mitochondria found in ultrathin sections, while only a few were freely dispersed in the hepatocyte cytoplasm. Lipid



droplets were not detected. Swollen mitochondria, lysosomes and autophagosomes were present in some hepatocytes.

Backcross *C. gibelio* × F1 hybrid (BC CaF1): the small, darkly pigmented MMCs were occasionally found in the liver tissue. The liver parenchyma was composed of markedly hypertrophic hepatocytes with considerable irregularity in size and containing almost colourless cytoplasm without granulation visible in HE and MT-stained sections (Figs. 3b and 4b). Their irregularly shaped nuclei and nucleoli were condensed, and the plasma membrane was distinct with irregular thickness. The pattern of glycogen-type vacuolisation observed in histological sections was similar to that in CaCa. The liver stained with AB-PAS confirmed very abundant glycogen with a similar distribution pattern to that observed in CaCa. The hepatocytes either had the glycogen concentrated at their peripheries and in rays surrounding the nucleus, or they showed very intense PAS staining evenly covering the entire cell (Fig. 4b). No lipid deposition was detected histologically, but several hepatocytes found in semithin and ultrathin sections contained single or clustered lipid droplets (staining blue in semithin sections). Under TEM, the hepatocytes showed a cytoplasm of medium density with unevenly distributed but abundant clusters of glycogen particles and dense granules, numerous mitochondria (with occasional swelling) and a relatively abundant RER accumulating in the perinuclear space and beneath the plasma membrane (Fig. 7e). The number of mitochondria and the RER lamellae that surrounded them differed between individual hepatocytes. Some areas of liver parenchyma consisted of hepatocytes with a significantly higher density of dense granules, giving the cytoplasm a much more granular appearance (less visible on histological sections). Irregularities of the plasma membrane observed in histological sections (Fig. 3b) were caused by focal accumulation of RER and mitochondria (Fig. 7e). Some hepatocytes contained one or two lipid droplets. Several autophagosomes were observed in hepatocytes, but lysosomes were rarely found in ultrathin sections.

Backcross F1 hybrid × *C. gibelio* (BC F1Ca): only a few darkly pigmented MMCs of various sizes (up to 80 µm) were found in the liver tissue. The liver parenchyma consisted of hypertrophic hepatocytes with wavy borders and cytoplasm showing mild granulation mainly concentrated around the nucleus (Fig. 3c). Their nuclei were condensed with irregular

nucleolus. The hepatocyte vacuolisation was of glycogen-type (Fig. 3c). The AB-PAS reaction revealed the highest glycogen content in liver parenchyma among all fish lines, with intense staining completely covering the hepatocytes (Fig. 4c). No lipid deposition was detected in histological or ultrathin sections, and semithin sections revealed only a few blue-stained lipid droplets occurring outside the hepatocytes. The TEM analysis of the hepatocytes showed that their cytoplasm with low electron density was packed with very abundant glycogen particles, numerous small clusters of dense granules with regular distribution, few peroxisomes, as well as massive RER surrounding the nucleus and several mitochondria (Fig. 7f). A thin layer of RER with focally adjacent mitochondria lined the cytoplasmic surface of the plasma membrane (Fig. 7f), giving hepatocytes a distinct and wavy border seen in histological sections (Fig. 3c). While most mitochondria showed clear signs of swelling, lysosomes and/or autophagosomes were observed in only a few hepatocytes.

Backcross *C. carpio* × F1 hybrid (BC CyF1): several small, darkly pigmented MMCs were observed in the liver tissue. The liver parenchyma consisted of hypertrophic hepatocytes that were irregular in shape and contained condensed nucleus and nucleolus (Figs. 5a and 6a). Their cytoplasm in HE- and MT-stained sections remained almost colourless and without granulation (Fig. 5a). The demarcation of hepatocytes by the plasma membrane was clearly visible but not completely continuous. Liver stained with AB-PAS showed a high glycogen content with irregular distribution (Fig. 6a). In most hepatocytes, the glycogen was concentrated peripherally and in radial protrusions around the nucleus, but in some hepatocytes, very intense staining uniformly covered almost the entire cell. While in histological sections, most of the hepatocytes showed distinct cytoplasmic vacuolisation of the glycogen type (similar to BC F1Ca), semithin and ultrathin sections revealed single tiny lipid droplets or large clusters of lipid droplets of various sizes in some hepatocytes. These were almost always coloured blue in semithin sections. The TEM analysis of hepatocytes revealed that their cytoplasm of low electron density was packed with abundant glycogen particles and numerous mitochondria (Fig. 7g). Individual hepatocytes contained glycogen particles of different sizes and uneven distribution. The long lamellae of the RER surrounded the large nucleus, with several branches surrounding the large mitochondria and ascending through the cytoplasm to the region below the hepatocyte plasma membrane. The number of



lipid droplets and the amount of glycogen particles and RER differed between individual hepatocytes. In addition, areas of liver parenchyma with normal hepatocytes alternated with areas with hepatocytes that had swollen mitochondria and showed obvious signs of cell damage. Lysosomes were commonly observed (mainly in damaged hepatocytes), while autophagosomes were rare.

Backcross F1 hybrid \times *C. carpio* (BC F1Cy): darkly pigmented MMCs of various sizes (up to 80 μ m) were commonly seen scattered throughout the liver tissue (Fig. 5b). The organisation of liver parenchyma differed from all studied fish lines (Figs. 5b and 6b). The hepatocytes were not hypertrophic and were similar in size to the hepatocytes of CyCy and F1 CaCy lines, but their cytoplasm was divided into granular and vacuolated regions, giving them a plastic appearance (Fig. 5b). Moreover, the granulated regions of hepatocyte cytoplasm appeared basophilic. The nuclei were large with condensed nucleolus. Histological sections revealed mild glycogen-type vacuolisation of hepatocyte cytoplasm. Liver stained with AB-PAS showed a moderate glycogen load with less intensively stained tissue at its periphery (Fig. 6b). Higher magnification revealed a cytoplasmic staining pattern similar to that of HE- or MT-stained hepatocytes, with unstained areas of cytoplasm alternating with intensely stained ones. Lipid deposition was not detected in hepatocytes in histological or ultrathin sections, but blue-stained lipid droplets occurring singly or in clusters within or outside the hepatocytes were seen in semithin sections. Under TEM, the hepatocyte cytoplasm was packed with very abundant glycogen particles (not wholly consistent with PAS reaction results) and numerous clusters of electron-dense granules with regular distribution (Fig. 7h). Hepatocyte cytoplasm also contained abundant mitochondria surrounded by several RER lamellae. The lamellae of RER with several mitochondria formed an irregular layer lining the cytoplasmic face of the plasma membrane, resulting in a clear demarcation of the hepatocyte. Furthermore, peroxisomes and large autophagosomes were present in most hepatocytes. The empty round areas (sometimes containing membranous remnants) (Fig. 7h) appear to correspond to the non-stained vacuolated areas in the cytoplasm of the PAS-positive hepatocytes (Fig. 6b).

F2 generation (F2): darkly pigmented MMCs of small to medium (up to 30 μ m) size were present in low numbers. The liver parenchyma contained polyhedral hepatocytes that were hypertrophic and

clearly demarcated by the plasma membrane (Figs. 5c and 6c). Like CaCa, the hepatocytes contained a more condensed nucleus, and their plasma membrane was less wavy. In MT-stained sections, the cytoplasm of hepatocytes had a slightly red tint, while the HE-staining appeared less intense compared to other fish lines (Fig. 5c). The pattern of glycogen-type vacuolisation observed in histological sections was similar to that of the CaCa and BC CaF1 lines, as well as the BC CyF1 line although less distinct in this case. Liver stained with AB-PAS showed a high glycogen load with a slightly uneven distribution in the tissue (Fig. 6c). The PAS staining pattern was similar to that of BC CyF1 and BC CaF1. Most of the hepatocytes contained glycogen accumulated mainly at their periphery and radially around the nucleus, while few showed an intense PAS reaction covering the entire cell (Fig. 6c). In terms of hepatocyte size and shape, overall appearance, and glycogen distribution, liver parenchyma most closely resembled that of BC CyF1. Semithin and ultrathin sections occasionally showed the presence of lipid droplets (more or less blue coloured in semithin sections) in hepatocytes. The TEM analysis revealed that the low-density cytoplasm of hepatocytes was packed with abundant glycogen particles and interspersed electron-dense granules, numerous large mitochondria, and massive RER (Fig. 7i). The electron-dense granules, as well as the glycogen particles of different sizes formed clusters, and their cytoplasmic distribution was slightly uneven. Similarly, the distribution of RER lamellae and mitochondria in the cytoplasm was uneven, with higher accumulation in the perinuclear space and often on one side of the hepatocyte. The cytoplasmic surface of the plasma membrane was lined with the RER lamellae and, in places, adjacent mitochondria (Fig. 7i), resulting in a distinct demarcation of hepatocytes seen in histological sections (Fig. 5c). No lipid droplets were observed in the cytoplasm of hepatocytes. Hepatocytes often contained large lysosomes and/or autophagosomes, as well as swollen mitochondria.

Spleen

The spleen of the studied fish lines did not show obvious macroscopic differences. The spleen-somatic indexes (SSI, mean \pm SD) for all fish lines are shown in Table 3.

In all fish lines, the histological analysis (HE and MT staining) revealed the presence of a thin capsule surrounding the spleen, trabeculae penetrating into the parenchyma, as well as other major splenic structures of higher vertebrates, such as red and white



pulps, blood vessels and ellipsoids (termination of splenic arterioles). However, the splenic parenchyma of all fish studied lacked nodular organisation and no border between the red and white pulp was observed (Figs. 8a-i and 9a-i). While white and red pulp were easier to distinguish at low magnification (Figs. 8a-i), higher magnification allowed the identification of specific cells (e.g. lymphocytes, erythrocytes, reticular cells, fibroblasts) and structures such as ellipsoids (Figs. 9a-i). The individual lines did not show significant deviations in the general architecture of the splenic parenchyma at low magnification in HE- (Figs. 8a-i; lower micrographs) and MT-stained sections. However, some differences could be observed in the organisation of the trabeculae and ellipsoids. The fibrous skeleton formed by trabeculae was most regularly arranged in the spleen of CyCy, followed by F1 CaCy, F1 CyCa and F2, and finally CaCa, BC CaF1, BC F1Ca, BC CyF1 and BC F1Cy. The trabeculae in CyCy, CaCa, F1 CaCy, BC CaF1, BC F1Ca, BC CyF1 and F2 were relatively thick, while those in F1 CyCa and BC F1Cy were thin. The ellipsoids were very prominent and numerous in CaCa and BC F1Ca, giving their parenchyma an island-like appearance (Fig. 8b and f), followed by F1 CaCy, F1 CyCa, BC CaF1, BC CyF1 and F2, while they were least numerous and distinct in CyCy and BC F1Cy. In F1 CyCa, BC CyF1 and F2, the MMCs were often present around the ellipsoids.

Surprisingly, parts of the spleen from all experimental fish lines (but not control wild fish) appeared haemorrhagic, with higher magnification revealing extravascular haemolysis accompanied by deposition of hematogenous pigments in the parenchyma. In addition to the degree of erythrocyte accumulation and haemolysis, the most significant differences were observed in the differentiation of hematogenous red pulp and lymphoid white pulp, the overall amount of white pulp, and the frequency of MMCs. The splenic parenchyma in all experimental fish lines, except CyCy, showed increased erythrocyte accumulation and massive haemolysis with yellow to brown pigment deposits present in at least a third of the spleen (Figs. 8b-i; upper micrographs). In CyCy, only a small portion of the splenic parenchyma showed light accumulation of yellow to rusty pigment indicative of ongoing mild haemolysis (Fig. 8a; upper micrograph). Moderate haemolysis with increased deposition of a rusty to brown pigment (presumed hemosiderin) was detected in the central parenchyma of BC CyF1 (Fig. 8g; upper micrographs). In the remaining fish lines, foci of deposited pigment gradually formed as a result of progressive haemolysis. Moderate to

severe, predominantly diffuse haemolysis in F2 and BC F1Ca (Figs. 8i, f; upper micrographs) and gradual formation of haemolytic foci in CaCa and BC CaF1 (Figs. 8b, e; upper micrographs) were accompanied by intense rusty pigmentation. Distinct foci of severe haemolysis with rusty to brown pigment depositions were found in the splenic parenchyma of F1 CaCy, F1 CyCa and BC F1Cy (Figs. 8c, d, h; upper micrographs). Regarding other pathological manifestations, few necrotic foci (mostly perivascular) were detected in the spleen parenchyma of F2, while these were relatively rare in CaCa (Fig. S1c), F1 CaCy (Fig. S1e), F1 CyCa, and BC F1Cy, and completely absent in CyCy, BC CaF1, BC F1Ca and BC CyF1.

The frequency and size of MMCs differed among the fish lines studied (Figs. 8 and S1). The lowest number of small MMCs (up to 60 μm) was observed in the spleen of BC CaF1 (Fig. 8e). This was followed by CaCa and F1 CaCy lines with small MMCs supplemented by several medium-sized (up to 100 μm) and distinct MMCs, and then CyCy with numerous MMCs that were of various sizes (up to 150 μm) and with a regular distribution throughout the splenic parenchyma (Figs. 8a-c and Figs. S1a, c, e). Next were F1 CyCa with small to medium-sized MMCs (up to 120 μm) regularly scattered throughout the tissue and BC F1Ca, which, although had fewer MMCs than F1 CyCa, these were very large (up to 260 μm) and compact (Figs. 8d, f). The BC CyF1, BC F1Cy and F2 lines had similar amounts of MMCs, which were predominantly medium-sized in BC CyF1 and BC F1Cy (up to 100 μm), whereas splenic parenchyma of F2 contained both medium- and large-sized (up to 200 μm) MMCs (Figs. 8g-i). The largest MMCs in the F2 line, present in non-haemolytic areas, were yellow in colour and compact (Fig. 8i). Overall, the largest and compact MMCs were almost always found in the non-haemolytic splenic parenchyma, while areas with ongoing or past haemolysis contained MMCs of smaller sizes and elongated shape.

Cell density in white pulp was evaluated in non-haemolytic parts of the spleen. After evaluating all sections from both staining methods, the cell density in white pulp appeared highest in CaCa and lowest in CyCy, F1 CaCy, F1 CyCa, BC CyF1, and BC F1Cy, with the least contrastingly coloured nuclei in CyCy, F1 CyCa and F1 CaCy (Figs. 8a-i). Approximately one-third of the spleen in BC F1Ca and CaCa was almost depleted of the erythrocytes (Figs. 8b, f; lower micrographs), with high magnification revealing an increased proportion of lymphocytes. In both HE- and MT-stained (Figs. 9a-i) sections of the spleen, evaluated



at high magnification, the violet areas outstanding at low magnification of HE-stained sections (Figs. 8a-i) were proved to be lymphocyte clusters, while scattered lymphocytes were also often detected. Histological sections of the spleens in CyCy, F1 CyCa and F2 showed erythrocytes of normal size, while the more or less haemolytic splenic parenchyma in other fish lines (F1 CaCy, BC CaF1, BC F1Ca, BC CyF1, CaCa, and BC F1Cy) contained clusters of enlarged erythrocytes and putative hemosiderin (Figs. 9a-i).

Discussion

Previous studies have shown that changes in fish physiology tend to manifest as histopathological alternations in certain organs, such as the gills and liver, and these tissues are suitable targets for evaluating the effects of pollutants or other adverse environmental factors, making them good indicators of water quality (Ghafarifarsani et al. 2023). In this study, we performed a detailed analysis of the architecture and possible histopathological abnormalities in two organs, the liver and spleen, which are crucial for metabolic and immune processes in fish, to evaluate the outcome of the hybridisation effects (Šimková et al. 2015, Sales et al. 2017). Previous studies demonstrated that the physiological, biochemical and immune parameters of F1 hybrids show an intermediate character between the parental species or were more similar to common carp, i.e. species in the paternal position (Šimková et al. 2015).

Liver

The architecture of a normal liver reflects not only its complex function but also many processes (physiological or pathological) taking place in other organs, as well as metabolic adaptations to dietary changes and environmental conditions. While it is one of the key organs in toxicological studies on vertebrates, interpretation of microscopic liver findings in fish is often challenging (Wolf & Wheeler 2018). Our observations agree with the general presumptions that lobules in the teleost liver are not defined compared with those in higher vertebrates (Akiyoshi & Inoue 2004, Mokhtar 2018). As already hypothesised for zebrafish, the liver lobes in fish could fulfil the function of mammalian hepatic lobules (Hardman et al. 2007, Yao et al. 2012). An in-depth analysis of 200 teleost livers confirmed a considerable variability in their histological features, and all of them differed from the image of mammalian livers (Akiyoshi & Inoue 2004). Their study classified the fish hepatocyte-sinusoidal structures into three types (cord-like, tubular and solid form) and hypothesises that during fish evolution, the

parenchymal arrangement progressed from solid or tubular form to cord-like form, with the hepatocytes changing from round to square and polyhedral cells. While in the cord-like form, most of the hepatocyte lining is single-layered (polyhedral hepatocytes with a round nucleus), in the tubular form, it is double-layered (polyhedral or round with a round nucleus). In solid form, the majority of the hepatocyte lining is multi-layered, with hepatocytes being round with a small round nucleus (Akiyoshi & Inoue 2004). The arrangement of the parenchyma in all fish lines studied in this work corresponds to the tubular form. In general, the appearance and organisation of hepatocytes in the liver parenchyma in pure lines of common carp and gibel carp were consistent with other studies (Mitsoura et al. 2013, Zhao et al. 2021, Uyisenga et al. 2023).

Two types of hepatocytes, lipid-rich and glycogen-rich, occur in teleost livers, with one predominant in each species (Akiyoshi & Inoue 2004). Fish hepatocytes are generally more vacuolated than mammalian ones due to higher glycogen and/or lipid contents compared to mammals (Wolf & Wolfe 2005). In addition to AB-PAS staining of histological sections, we subjected the liver to TEM analysis to distinguish with greater certainty the glycogen or lipid nature of hepatocyte vacuolisation and to analyse the changes found in histological sections more deeply. Ultrastructural appearance of glycogen particles, lipid droplets, as well as major hepatocyte organelles or structures such as nucleus, mitochondria, RER and bile canaliculi corresponded to that in other fish species (Tanuma 1980, Rocha et al. 1994, Dyková et al. 2022).

Glycogen is a polysaccharide that stores carbohydrates and is especially abundant in the liver and muscle tissue. It represents a labile, readily available, but energy-intensive compound that can be converted to glucose at critical times, such as when toxins enter fish tissues or in anoxic conditions (Makarenko et al. 2022). For example, a reduced number of glycogen particles was demonstrated in the hepatocytes of starved fish, with low glycogen levels remaining after 30 days of refeeding (Souza et al. 2001). Gibel carp keeps the largest glycogen stores among vertebrates (25-30% of the liver being glycogen), enabling it to survive anoxia for prolonged periods (Hochachka & Somero 1984, De Boeck et al. 2010, Fuad et al. 2021). A strong reaction of hepatocytes with PAS and Best's carmine has also been reported in other cyprinids, for example, in grass carp *Ctenopharyngodon idella* (Mokhtar 2018). However, compared to other



fish species, the quantity of glycogen particles in *Carassius* spp. liver is two times higher (Balashov & Recoubratsky 2011). Our observations agree with this fact, since the hepatocytes in all fish lines analysed in this study, except the CyCy line (pure *C. carpio*), were glycogen-rich with glycogen-type vacuolisation. The highest glycogen load we observed in hepatocytes of F1 CyCa (F1 with *C. carpio* mtDNA), BC F1Ca and BC CaF1 (maternal backcrosses), followed by BC CyF1 (paternal backcross), F2 (both parents being F1 hybrids with *C. gibelio* mtDNA) and CaCa (pure *C. gibelio*), and then BC F1Cy (paternal backcross) and F1 CaCy (F1 with *C. gibelio* mtDNA). Thus, it is clear that compared to CyCy, the genomic contribution of gibel carp led to an increase in the amount of glycogen in the liver tissue of all progeny lines. The lowest glycogen load in the CyCy liver parenchyma contradicts the results of PAS staining in another study (Giari et al. 2016). However, in the mentioned study, the hepatocytes in all studied individuals of common carp showed foamy vacuolisation (similar to that observed in hepatocytes of CaCa and hybrid fish in our study), which is not characteristic of *C. carpio* liver (Mitsoura et al. 2013, Emadi et al. 2018, Korkmaz et al. 2020). Similar hepatocyte vacuolisation was induced in common carp fed a high-fat and high-carbohydrate diet (Yang et al. 2023), which was confirmed by another study demonstrating that different types of diets influence the vacuolisation and pathological alterations of liver parenchyma (Yang et al. 2019). Since the common carp is an omnivorous fish, individuals fed a mixed (animal and vegetable) diet showed stronger antioxidant capacity and liver parenchyma with an almost normal appearance (Yang et al. 2019). Moreover, numerous abiotic and biotic factors may influence the accumulation of glycogen and lipids in fish tissues. One of them is the reproductive cycle of female fish (Jordanova et al. 2016a). In our study, no fish line showed a significant increase in liver fat deposition (Table 3), confirming that the experimental fish were not exposed to nutritional stress (Ruiz-Ramírez et al. 2019). Although we observed the highest number of lipid droplets in liver parenchyma of CyCy, these were only observable in ultrathin sections or semithin sections stained with toluidine blue, but not in histological sections. Semithin sections stained with toluidine blue proved to be much more sensitive when comparing the liver fat content across fish lines, as the lipid droplets stained light or steel blue and were, therefore, easily distinguished from the surrounding purple liver tissue. Accordingly, the electron density of lipid droplets in ultrathin sections varied from light to dark grey with an osmiophilic contour, reflecting

their saturation degree, as saturated lipids do not react with OsO_4 and remain translucent (Hayat 2000). Interestingly, no lipid droplets were detected in the liver parenchyma of the CaCa line despite its fatty-like appearance in HE-stained histological sections.

Various causes, including the accumulation of glycogen, lipids and water, as well as the proliferation of cellular organelles, can lead to the enlargement of hepatocytes (Rosenthal et al. 1984, Wolf & Wolfe 2005). Hepatocytes hypertrophied due to exposure to pollutants typically show excessive lipid accumulation and endoplasmic reticulum proliferation (Rosenthal et al. 1984). Hepatocyte hypertrophy, giving the affected cells a pale, ground glass appearance (Gopinath et al. 1987), was most pronounced in BC CaF1, followed by BC F1Ca and CaCa, and finally BC CyF1 and F2. However, contrary to the general assumptions discussed in some works (Wolf & Wolfe 2005), the hepatocyte hypertrophy observed in this study did not correspond to an increase in HSI nor to the proliferation of specific organelles or cytoplasmic inclusions (Table 3). Although hepatocellular hypertrophy usually occurs after exposure to xenobiotic agents that cause induction of liver enzymes, physiological hepatocyte hypertrophy can be observed in reproductively active female fish or male fish exposed to exogenous estrogenic compounds (Gopinath et al. 1987, Wolf & Wolfe 2005). Since in our study, all fish were reared under the same experimental conditions and hepatocyte hypertrophy was observed in both females and males, we hypothesise that this is the physiological state of hepatocytes characteristic of the given fish lines.

The liver parenchyma showed similarities in some fish lines, especially in the organisation and shape of hepatocytes, their size and overall appearance, hepatocyte demarcation and degree of hypertrophy, condensation of nuclei/nucleoli, vacuolisation pattern and glycogen content. Accordingly, these fish lines also showed the similar fine structure of hepatocytes, particularly in terms of the granularity of their cytoplasm, the number of glycogen particles, the appearance and size of the nucleus, as well as the amount and accumulation of RER lamellae and mitochondria in the perinuclear space and beneath the plasma membrane. From this point of view, the liver parenchyma of CyCy was most similar to F1 CaCy and partly to BC F1Cy (with hepatocytes having significantly less granulated cytoplasm), suggesting the significance of the genomic contribution of the fish species in the paternal position (in this case



common carp). However, this trend did not match the situation in the other fish lines, as the liver parenchyma of CaCa was most similar to BC CaF1 and slightly less similar to BC F1Ca (hepatocytes with more granulated cytoplasm) and F2 generation (less hypertrophied hepatocytes), while the liver parenchyma of F1 CyCa and BC CyF1 shared the features of both groups.

Interestingly, the liver of all fish lines showed histopathological changes, such as sinusoidal congestion, fibrosis and necrosis. The signs of liver necrosis were found in all fish lines and were always accompanied by parenchymal regeneration, indicating a chronic process. The ultrastructure of hepatocytes and potential alternations in their subcellular organisation could only be verified in pure lines of common carp and gibel carp, but not in hybrid fish lines, which have not yet been studied from this point of view. As far as we can evaluate based on the published data (very limited and often inconsistent), the subcellular organisation of hepatocytes in the CyCy and CaCa lines is consistent with that documented in other studies on common carp and gibel carp (e.g. Braunbeck & Appelbaum 1999, Zhang et al. 2021, Gao et al. 2023). However, the hepatocytes of both fish lines showed some abnormalities. In CyCy hepatocytes, the RER lamellae sheathing abundant mitochondria were irregularly arranged, and some appeared fragmented, with autophagosomes commonly present in our specimens indicating hepatocellular pathology. In addition to the disorderly arranged and fragmented RER lamellae, the hepatocytes of CaCa frequently showed mitochondrial swelling. These subcellular changes in fish liver have been often attributed to various agents such as pesticides, herbicides and other water pollutants (Peters et al. 1987, Grund et al. 2010), heavy metals and metal nanoparticles (Franchini et al. 1991, Diniz et al. 2013, Naguib et al. 2020), cyanobacterial toxins (Li et al. 2005, Drobac et al. 2016), microbial infections (Almendras et al. 2000, Kent & Myers 2000), transport anoxia, and hypoxic conditions in rearing tanks (Speare 2000). Nevertheless, these were usually accompanied by other liver alternations not detected in our study, such as haemorrhage, increase in MMCs, glycogen depletion, fatty degeneration, frequent nuclear changes, RER vesiculation and proliferation of the smooth endoplasmic reticulum (e.g. Kent & Myers 2000, Grund et al. 2010, Li et al. 2021). It is important to mention that we did not detect any microbial infection in the liver tissue of experimental fish analysed by electron microscopy. Similar liver pathology can also be induced by certain diets, such as

a high-starch diet, which has been shown to promote synthesis and excessive accumulation of glycogen, leading to significant tissue damage manifested by vacuolar degeneration, sinusoidal congestion with inflammatory cell infiltration, and moderate to severe necrosis (Zhong et al. 2022). Since the necrotic foci observed in the experimental fish were associated with relatively little or no inflammation, we consider the hepatic necrosis to be bland and caused by direct liver damage, most likely due to stopped or slowed blood flow (ischemia). For example, hepatic infarction or ischemic hepatitis (also known as hypoxic hepatitis or shock liver; Ebert 2006, Spengler & Fontana 2018) are not mediated by an inflammatory process. In the ischemic liver, the hepatocytes are damaged by chronic recurrent hypoxic conditions and increased sinusoidal pressure (Ebert 2006). This condition might be related to profound anaemia (Okas et al. 2001). However, it should be mentioned that liver necrosis is reported to be quite common in fish, and its increased occurrence in gibel carp has been recorded in autumn (Kurchenko et al. 2021). Accordingly, control wild fish in our study also showed liver necrosis, with the mildest form (diffuse patchy necrosis) in common carp and the most severe (multifocal necrosis) in the F1 generation. Interestingly, even among the experimental fish lines, pure common carp showed the mildest form of liver necrosis.

Spleen

The immune system of fish considerably differs from that of mammals, mainly due to the lack of bone marrow and lymph nodes. Instead, the kidney plays the role of the main lymphoid organ in fish, along with the spleen, thymus, and mucosa-associated lymphoid tissues (Press & Evensen 1999), with the spleen considered the major secondary lymphoid organ (Sayed et al. 2022). It was suggested that the immunocompetence of fish may be determined by the emergence of immunological capacities rather than the histological maturation of lymphoid organs (Zapata 2024). Accordingly, the adult teleost spleen usually shows poorly developed lymphoid tissue scattered throughout the reticular splenic parenchyma surrounding small arteries and MMCs, but the splenic lymphoid tissue increases significantly after antigenic stimulation (Zapata 2024). The splenic tissue of fish does contain red and white pulp, but unlike the spleen of mammals, there are no boundaries between them. The white pulp, formed by lymphoid tissue, surrounds small arteries and diffusely intermeshes with the red pulp. Blood filtration occurring through sheets of leukocytes of the white pulp (lymphoid tissue) is released in the red pulp, composed only



of the peripheral blood surrounding the white pulp (Bjørgen & Koppang 2021). The relative volumes of red and white pulp in fish are known to change throughout their reproductive cycle, with white pulp increasing significantly and red pulp decreasing from pre-vitellogenesis to spawning. The opposite trend occurs towards post-spawning (Rebok et al. 2011).

Our observations of splenic parenchyma in all fish lines are consistent with published works which, with a few exceptions, report the absence of the typical nodular organisation of fish splenic parenchyma with barely discernible boundaries between white and red pulp (Marancik et al. 2014, Sales et al. 2017, Dyková et al. 2022). However, in contrast to other fish (Ruiz et al. 2020), cyprinid fish used in our study appear to have fewer trabeculae. Moreover, although the collagen fibres around the muscles were intensely stained green with MT, the connective tissue in splenic trabeculae showed only very faint green staining in all specimens (Figs. 9a-i), suggesting that the fibrous skeleton of the fish spleen may contain less collagen and more reticular fibres. The histoarchitecture of the spleen of the studied fish lines did not differ significantly, although some differences were documented. For example, the spleen of CaCa showed an irregular organisation of the fibrous skeleton (the most collagen-rich of all fish lines) with thick but short trabeculae, the most numerous and prominent ellipsoids, and the highest cell density in the white pulp. In contrast, the most regular organisation of the fibrous skeleton was observed in CyCy, accompanied by indistinct ellipsoids and white pulp with the lowest cell density.

Surprisingly, at least part of the spleen in all experimental fish lines examined in this study exhibited extensive parenchymal areas with marked accumulation of erythrocytes and haemolysis accompanied by increased deposition of hematogenous pigments. From these, only CyCy showed mild haemolysis confined to a relatively small part of the spleen, followed by BC CyF1 with moderate haemolytic changes in splenic parenchyma. Abundant hemosiderin, produced by the degradation of haemoglobin, as well as aggregates of pigmented macrophages, are often detected during haemolytic anaemia (Wolke 1992, Agius & Roberts 2003, Kasprzak et al. 2023), a blood disorder caused by a variety of factors such as vitamin B deficiency, viral and bacterial infections, haemoparasites, and intoxication with various substances including cyanotoxins (Clauss et al. 2008, Zhou et al. 2012, Witeska 2015). A haemolytic effect has also been described in the

bacterial pathogen *Aeromonas*, often associated with haemorrhages in fish internal organs, but infected individuals also show other signs of systemic infection (Abdelhamed et al. 2017, Baumgartner et al. 2017, Bakiyev et al. 2023).

Besides significant haemolysis, we detected enlarged erythrocytes in some fish lines (CaCa, F1 CaCy, BC CaF1, BC F1Ca, BC CyF1, and BC F1Cy). Enlarged erythrocytes may be related to macrocytic anaemia, toxins, bacteria, parasites, and hypoxia but may also reflect chronic liver disease (Agarwal et al. 1984). For example, cyprinid fish (including *C. carpio*) can develop macrocytic anaemia due to stress and reduced food supply, for example, due to competition for food (Roy George et al. 2015). However, macrocytosis can also be associated with haemolytic anaemia and/or anaemia recovery (Kaferle & Strzoda 2009). Similar to common carp or other fish exposed to heavy metals or chemicals (David & Kartheek 2015, Abu Zeid et al. 2021, Farhan et al. 2021), we observed an intensification of red pulp with increasing hemosiderosis and increasing numbers of dark brown melanomacrophages (aggregating into MMCs), accompanied by white pulp depletion with disappearance of large MMCs. Mild necrosis observed in splenic parenchyma of some experimental fish lines may also be related to anaemia (Noyes et al. 1991). In contrast, no extravascular haemolysis (Fig. S1a) or necrotic changes were found in the splenic parenchyma of wild control fish, except for a single individual of gibel carp, whose spleen had a small necrotic area with mild fibrotic changes indicating a reparative process (Fig. S1d).

It is almost impossible for experimental fish maintained in aquaria with settled tap water under controlled conditions to become intoxicated by chemicals or heavy metals or to become infected with pathogens commonly found in aquacultures. In addition, live fish showed no visible signs of chronic or acute disease, and we did not observe macroscopic changes in the internal organs during their dissection. We, therefore, consider a monotonous diet (e.g. vitamin B deficiency) or specific tap water parameters (such as high hardness or unsuitable pH) as possible factors. Although the mixed diet comprising dried pellets and flakes enriched by frozen adult *Artemia* should cover the nutritional requirements, the vitamins might be less available due to the lower digestibility (Mæland et al. 2000). However, it seems more likely that the fish were not comfortable with long-term (three years) breeding in tap water in the limited space of the aquarium. Variations in



physicochemical parameters, such as pH and water hardness, are known to induce oxidative stress in fish (Menon et al. 2023). The tap water in Brno is considered hard on the water hardness scale. Currently, the tap water in the area of our laboratory has a hardness of 2.8 mmol/L (corresponding to 280.25 mg CaCO₃/L) and a pH of 7.46 (Brněnské vodárny a kanalizace 2024, <https://www.bvk.cz/pitna-voda/kvalita-vody>). For fish cultivation, water hardness in the range of 50-150 mg/L of CaCO₃ is considered desirable (most preferably above 100 mg/L), while above 300 mg/L, it has been found to be lethal for fish (Swain et al. 2020). It has been shown that chronic exposure of fish to elevated water hardness can result in a significant decline in the haemoglobin content and haematocrit, indicating the development of anaemic conditions (Limbaugh et al. 2021). In both acidic and alkaline environments, cyprinid fish might experience the distortion and lysis of red blood, which can be compensated at intermediate pH values (i.e. pH 6.5 and 8.5) by the production of immature erythrocytes through stimulated haemopoiesis, and the fish then suffer from haemolytic anaemia (Das et al. 2006, Ghanbari et al. 2012). While the optimum pH range differs among fish species, the best pH range for common carp survival and growth is between 7.5 and 8.0 (Heydarnejad 2012). At the time we conducted the experiments, the tap water in our laboratory had a pH of 7.2 ± 0.2, which is slightly more acidic than the optimum range mentioned above. It is also worth noting that an unfavourable pH can also negatively affect the efficiency of the use of nutrients from food.

The melanomacrophage centres

The MMCs, composed of specialised cells of the innate immune system, are polymorphic structures most often present in the spleen, kidneys and sometimes liver of fishes, but they can also be found in other organs, especially in connection with inflammation (Wolke 1992). Simply put, they represent a focal accumulation of pigment-containing macrophages, enlarging after active phagocytosis of heterogeneous materials (Agius & Roberts 2003). The MMCs perform various functions, including recycling, storing and detoxifying cellular wastes and exogenous substances and focal deposition for resistant intracellular bacteria (Montero et al. 1999, Agius & Roberts 2003). Since in higher teleosts, they rather represent complex discrete centres containing lymphocytes and macrophages, they are considered primitive analogues of the germinal centres of lymph nodes (Agius & Roberts 2003). The MMCs of fish, increasing in size or frequency under environmental

stress, could serve as biomarkers of water quality in terms of deoxygenation and iatrogenic chemical pollution (Agius & Roberts 2003). Aquaculture studies have linked the increase in MMC size to stress and inflammation (Kasprzak et al. 2023). The number and size of MMCs, along with their pigment contents, vary with fish health and environmental degradation, and it has been suggested that increased numbers of MMCs in the fish spleen are induced by stress and environmental factors rather than by tissue catabolism (Sayed et al. 2022). Nevertheless, the occurrence of MMCs in fish hematopoietic tissues is also influenced by other factors, such as fish age or sex, vitamin deficiency, starvation, disease process and bleeding (Montero et al. 1999, Mikula et al. 2008, Jordanova et al. 2016b). For example, while starved or stressed fish tend to show increased density of splenic MMCs, a reduction in MMCs size and number has been reported in fish from polluted environments, possibly due to pollutant-induced immunosuppression (De Vico et al. 2008). As a result, wild fish seem to have fewer MMCs than farmed fish (Kurtović et al. 2008). Although MMCs are generally considered to be a broadly applicable histological indicator of fish immune and health status as well as overall well-being, this may not be the case in all fish species as it is not entirely clear how these structures respond to various stimulating or stressing factors (Steinel & Bolnick 2017, Kasprzak et al. 2023, Passantino et al. 2024).

In the fish spleen, the melanomacrophages were reported to be arranged either in clusters or more loosely dispersed within the white pulp, depending on species. Apart from erythrocyte fragments, these phagocytic cells contain various pigments such as melanin, ceroid, hemosiderin, and lipofuscin localised in vacuoles, which increase in volume and range in older fish or because of a cachectic disease (Agius & Roberts 2003, Mikula et al. 2008, Sayed et al. 2022). Hemosiderin is related to iron storage and recycling, while ceroid and lipofuscin originate from cell/organelle peroxidation and melanin may play a role in defence mechanisms (Montero et al. 1999). The fact that splenic MMCs are storage sites for blood breakdown products such as hemosiderin and lipofuscin (De Vico et al. 2008) also explains their high occurrence in haemolytic lesions found in the splenic parenchyma of experimental fish in our study. Hemosiderin distribution in teleosts appears to be restricted mainly to the splenic MMCs, and it is possible that only these are normally involved in hemosiderin handling in both healthy and diseased



fish (Agius & Roberts 2003). The association between haemolytic anaemia and increased deposition of haemosiderin in MMCs was reported in previous studies (Roberts & Rodger 2012, Pronina et al. 2014, Manrique et al. 2019).

The differences observed in the MMCs between individual experimental fish lines studied in our work are not surprising, as MMCs were shown to vary between species (Agius & Roberts 2003). However, we also observed differences between the wild and experimental fish of the same species. The spleen of wild *C. carpio* (Fig. S1b) had larger and more compact MMCs compared to the experimental line of pure *C. carpio* (CyCy; Fig. S1a), while the hepatic MMCs were more abundant in experimental fish. The pigment detected in the spleen of wild *C. carpio* was rusty in colour, while the splenic parenchyma of the experimental fish contained dark brown pigment dispersed in smaller clusters (Figs. S1a, b). The spleen in the experimental line of pure *C. gibelio* (CaCa) had more frequent MMCs (Fig. S1c) when compared to wild *C. gibelio* individuals (Fig. S1d). The deposited pigment was again of rusty colour in wild fish. The hepatic MMCs were extremely rare in both the wild and experimental *C. gibelio*. A different situation occurred in F1 hybrids with *C. gibelio* mtDNA (Figs. S1e, f). While the laboratory-bred F1 hybrids (F1 CaCy) exhibited numerous and variously sized MMCs with dark brown pigment (Fig. S1e), histological examination of wild individuals revealed significant variability in the frequency and size of splenic MMCs (Fig. S1f). One of the three fish examined had a spleen with abundant and variously sized MMCs with brown pigment, while the other had only a few medium-sized MMCs with rusty to brown pigment, and the third had almost no MMCs with light, yellow-brown pigment. In contrast, liver parenchyma showed no significant differences in the number or size of MMCs between experimental and wild F1 hybrids. Our observations are consistent with the general assumption that, compared to the spleen, hepatic MMCs are known to be smaller and less numerous (Kasprzak et al. 2023). Moreover, changes in MMCs are likely to occur earlier in the liver than in the spleen, and small MMCs might disappear due to their atrophy or emigration from the liver (Kasprzak et al. 2023). The differences in the number and appearance of MMC between the wild and experimental fish of the same species in our study most likely arose as a result of massive haemolysis, during which the number of dark brown melanomacrophages forming small aggregations increases and large MMCs disappear (David &

Kartheek 2015, Abu Zeid et al. 2021, Farhan et al. 2021). Similar differences were observed between haemolytic and non-haemolytic splenic parenchyma of experimental fish, the latter containing significantly larger and more compact MMCs.

Conclusions

While the organisation of liver and spleen parenchyma did not show a clear trend based on the type of crossbreeding representing the different genomic contributions of common carp and gibel carp, some similarities could be observed between certain fish lines. Differences in the liver were most evident in the specific properties of hepatocytes, the pattern of glycogen distribution in their cytoplasm, and in the spleen in the organisation of trabeculae and ellipsoids. Moreover, this study revealed pathological changes in all experimental fish lines, particularly significant extravascular haemolysis in the splenic parenchyma and foci of hepatic necrosis observed mainly at the periphery of the liver parenchyma. After considering the possible factors known to lead to such pathological manifestations, we assume that the haemolysis developed in experimental fish as a result of long-term breeding in settled and aerated tap water, which, although commonly used for experiments on freshwater fish, may not have the most suitable parameters for the normal physiology of wild species. The chronic haemolysis could lead to an anaemic state and hypovolaemic hypotension, causing necrosis of the liver parenchyma. Compared to invasive gibel carp and hybrid lines, common carp with a longer history of cultivation coped best with these artificial conditions and showed the mildest forms of observed pathologies.

Acknowledgements

This study was funded by Czech Science Foundation, project no. 19-10088S. We are greatly indebted to Gabriela Vágnerová from Faculty of Science, Masaryk University, Brno for processing the samples for histological analysis. We acknowledge the BC CAS core facility LEM supported by the Czech-BioImaging large RI project (LM2018129 and OP VVV CZ.02.1.01/0.0/0.0/18_046/0016045 funded by MEYS CR) for their support with obtaining the TEM data presented in this paper.

Author Contributions

A. Šimková conceived and designed the fish hybridisation study. A. Valigurová and I. Hodová designed and carried out the histopathological and ultrastructural analyses. L. Vetešník



performed field sampling, carried out fish manipulation and artificial breeding, dissected fish and collected tissues for further analyses. A. Valigurová prepared the first draft and

final version of the manuscript. A. Šimková, L. Vetešník and I. Hodová revised the first version of the manuscript. All authors read and approved the final version of the manuscript.



Literature

- Abdelhamed H., Ibrahim I., Baumgartner W. et al. 2017: Characterization of histopathological and ultrastructural changes in channel catfish experimentally infected with virulent *Aeromonas hydrophila*. *Front. Microbiol.* 8: 1519.
- Abu Zeid E.H., Khalifa B.A., Said E.N. et al. 2021: Neurobehavioral and immune-toxic impairments induced by organic methyl mercury dietary exposure in Nile tilapia *Oreochromis niloticus*. *Aquat. Toxicol.* 230: 105702.
- Agarwal V.P., Goel K.A., Kalpana S. et al. 1984: Alachlor toxicity to a freshwater teleost *Clarias batrachus*. *Curr. Sci.* 53: 1050–1052.
- Agius C. & Roberts R.J. 2003: Melano-macrophage centres and their role in fish pathology. *J. Fish Dis.* 26: 499–509.
- Akiyoshi H. & Inoue A. 2004: Comparative histological study of teleost livers in relation to phylogeny. *Zool. Sci.* 21: 841–850.
- Almendras F.E., Fuentealba I.C., Markham R.F.F. et al. 2000: Pathogenesis of liver lesions caused by experimental infection with *Piscirickettsia salmonis* in juvenile Atlantic salmon, *Salmo salar* L. *J. Vet. Diagn. Inv.* 12: 552–557.
- Arnold M.L. & Hodges S.A. 1995: Are natural hybrids fit or unfit relative to their parents? *Trends Ecol. Evol.* 10: 67–71.
- Bakiyev S., Smekenov I., Zharkova I. et al. 2023: Characterization of atypical pathogenic *Aeromonas salmonicida* isolated from a diseased Siberian sturgeon (*Acipenser baerii*). *Heliyon* 9: e17775.
- Balashov D.A. & Recoubatsky A.V. 2011: Hypoxia tolerance of hybrids of carp *Cyprinus carpio* and golden carp *Carassius auratus*. *J. Ichthyol.* 51: 641–645.
- Bartley D.M., Rana K. & Immink A.J. 2000: The use of inter-specific hybrids in aquaculture and fisheries. *Rev. Fish Biol. Fish.* 10: 325–337.
- Baumgartner W.A., Ford L. & Hanson L. 2017: Lesions caused by virulent *Aeromonas hydrophila* in farmed catfish (*Ictalurus punctatus* and *I. punctatus* × *I. furcatus*) in Mississippi. *J. Vet. Diagn. Invest.* 29: 747–751.
- Berillis P., Mente E. & Nengas I. 2011: Collagen fibrils in cultured and wild sea bream *Sparus aurata* liver. An electron microscopy and image analysis study. *Sci. World J.* 11: 538413.
- Bjørgen H. & Koppang E.O. 2021: Anatomy of teleost fish immune structures and organs. *Immunogenetics* 73: 53–63.
- Braunbeck T. & Appelbaum S. 1999: Ultrastructural alterations in the liver and intestine of carp *Cyprinus carpio* induced orally by ultra-low doses of endosulfan. *Dis. Aquat. Org.* 36: 183–200.
- Burke J.M. & Arnold M.L. 2001: Genetics and the fitness of hybrids. *Annu. Rev. Genet.* 35: 31–52.
- Clauss T.M., Dove A.D.M. & Arnold J.E. 2008: Hematologic disorders of fish. *Vet. Clin. N. Am. Exot. Anim. Pract.* 11: 445–462.
- Copp G.H., Bianco P.G., Bogutskaya N.G. et al. 2005: To be, or not to be, a non-native freshwater fish? *J. Appl. Ichthyol.* 21: 242–262.
- Das P.C., Ayyappan S. & Jena J.K. 2006: Haematological changes in the three Indian major carps, *Catla catla* (Hamilton), *Labeo rohita* (Hamilton) and *Cirrhinus mrigala* (Hamilton) exposed to acidic and alkaline water pH. *Aquaculture* 256: 80–87.
- David M. & Kartheek R.M. 2015: Histopathological alterations in spleen of freshwater fish *Cyprinus carpio* exposed to sublethal concentration of sodium cyanide. *Open Vet. J.* 5: 1–5.
- De Boeck G., Smolders R. & Blust R. 2010: Copper toxicity in gibel carp *Carassius auratus gibelio*: importance of sodium and glycogen. *Comp. Biochem. Physiol. C Toxicol. Pharmacol.* 152: 332–337.
- De Vico G., Cataldi M., Carella F. et al. 2008: Histological, histochemical and morphometric changes of splenic melanomacrophage centers (Smmcs) in *Sparicotyle*-infected cultured sea breams (*Sparus aurata*). *Immunopharmacol. Immunotoxicol.* 30: 27–35.
- Diniz M.S., de Matos A.P.A., Lourenço J. et al. 2013: Liver alterations in two freshwater fish species (*Carassius auratus* and *Danio rerio*) following exposure to different TiO₂ nanoparticle concentrations. *Microsc. Microanal.* 19: 1131–1140.
- Drobac D., Tokodi N., Lujić J. et al. 2016: Cyanobacteria and cyanotoxins in fishponds and their effects on fish tissue. *Harmful Algae* 55: 66–76.
- Dyková I., Žák J., Blažek R. et al. 2022: Histology of major organ systems of *Nothobranchius* fishes: short-lived model species. *J. Vertebr. Biol.* 71: 21074.
- Ebert E.C. 2006: Hypoxic liver injury. *Mayo Clin. Proc.* 81: 1232–1236.
- Emadi H., Shariatzadeh S., Jamili S. et al. 2018: Evaluation of toxicity and biochemical effects of the oxadiargyl in common carp (*Cyprinus carpio* L.). *Int. J. Aquat. Biol.* 6: 55–60.
- Farhan M., Wajid A., Hussain T. et al. 2021: Investigation of oxidative stress enzymes and



- histological alterations in tilapia exposed to chlorpyrifos. *Environ. Sci. Pollut. Res. Int.* 28: 13105–13111.
- Franchini A., Barbanti E. & Fantin A.M.B. 1991: Effects of lead on hepatocyte ultrastructure in *Carassius carassius* (L.) var. *auratus*. *Tissue Cell* 23: 893–901.
- Fuad M.M.H., Vetešník L. & Šimková A. 2021: Is gynogenetic reproduction in gibel carp (*Carassius gibelio*) a major trait responsible for invasiveness? *J. Vertebr. Biol.* 70: 21049.
- Gao X., Ma C., Wang H. et al. 2023: Multi-walled carbon nanotube induced liver injuries possibly by promoting endoplasmic reticulum stress in *Cyprinus carpio*. *Chemosphere* 325: 138383.
- Ghafariarsani H., Raeeszadeh M., Hajirezaee S. et al. 2023: The effect of malathion concentration and exposure time on histopathological changes in the liver and gill of rainbow trout. *Aquac. Res.* 2023: 3396066.
- Ghanbari M., Jami M., Domig K. et al. 2012: Long-term effects of water pH changes on hematological parameters in the common carp (*Cyprinus carpio* L.). *Afr. J. Biotechnol.* 11: 3153–3159.
- Giari L., Vincenzi F., Badini S. et al. 2016: Common carp *Cyprinus carpio* responses to sub-chronic exposure to perfluorooctanoic acid. *Environ. Sci. Pollut. Res. Int.* 23: 15321–15330.
- Gopinath C., Prentice D.E. & Lewis D.J. 1987: The liver. In: Gopinath C., Prentice D.E. & Lewis D.J. (eds.), *Atlas of experimental toxicological pathology*. Springer, Dordrecht, Netherlands: 43–60.
- Grund S., Keiter S., Böttcher M. et al. 2010: Assessment of fish health status in the Upper Danube river by investigation of ultrastructural alterations in the liver of barbel *Barbus barbus*. *Dis. Aquat. Org.* 88: 235–248.
- Hardman R.C., Volz D.C., Kullman S.W. et al. 2007: An *in vivo* look at vertebrate liver architecture: three-dimensional reconstructions from medaka (*Oryzias latipes*). *Anat. Rec. (Hoboken)* 290: 770–782.
- Hayat M. 2000: Principles and techniques of electron microscopy: biological applications, 4th ed. Cambridge University Press, Cambridge, UK.
- Heydarnejad M.S. 2012: Survival and growth of common carp (*Cyprinus carpio* L.) exposed to different water pH levels. *Turk. J. Vet. Anim. Sci.* 36: 245–249.
- Hochachka P.W. & Somero G.N. 1984: Biochemical adaptation. Princeton University Press, Princeton, USA.
- Humason G.L. 1967: Animal tissue techniques, 2nd ed. W.H. Freeman and Company, San Francisco, USA.
- Jordanova M., Rebok K., Malhão F. et al. 2016a: Seasonal changes in hepatocytic lipid droplets, glycogen deposits, and rough endoplasmic reticulum along the natural breeding cycle of female ohrid trout (*Salmo letnica* Kar.) – a semiquantitative ultrastructural study. *Microsc. Res. Tech.* 79: 700–706.
- Jordanova M., Rebok K., Naskovska M. et al. 2016b: Splenic pigmented macrophage aggregates in barbel (*Barbus peloponnesius*, Valenciennes, 1844) from river Bregalnica – influences of age, sex and season on a pollution biomarker. *Turk. J. Fish. Aquat. Sci.* 16: 881–890.
- Kaferle J. & Strzoda C.E. 2009: Evaluation of macrocytosis. *Am. Fam. Physician* 79: 203–208.
- Kasprzak R., Zakęs Z., Kamaszewski M. et al. 2023: Histomorphometric evaluation of melanomacrophage centers (MMCs) and CD3+ T cells of two morphs of brown trout (*Salmo trutta*) fed diets with immunostimulants. *Fish Shellfish Immunol.* 141: 109020.
- Kent M.L. & Myers M.S. 2000: Hepatic lesions in a redstriped rockfish (*Sebastes proriger*) suggestive of a herpesvirus infection. *Dis. Aquat. Org.* 41: 237–239.
- Korkmaz C., Ay Ö., Dönmez A.E. et al. 2020: Influence of lead on reproductive physiology and gonad and liver histology of female *Cyprinus carpio*. *Thalassas: Int. J. Mar. Sci.* 36: 597–606.
- Kurchenko V., Sharamok T. & Holub O. 2021: The histopathological condition of hepatopancreas of the Prussian carp (*Carassius gibelio* (Bloch, 1782)) in the modern conditions of the Zaporizhian (Dnipro) reservoir. *World Scientific News* 153: 181–191.
- Kurtović B., Teskeredžic E. & Teskeredžic Z. 2008: Histological comparison of spleen and kidney tissue from farmed and wild European sea bass (*Dicentrarchus labrax* L.). *Acta Adriat.* 49: 147–154.
- Li L., Xie P. & Chen J. 2005: *In vivo* studies on toxin accumulation in liver and ultrastructural changes of hepatocytes of the phytoplanktivorous bighead carp i.p. – injected with extracted microcystins. *Toxicon* 46: 533–545.
- Li H., Xu W., Wu L. et al. 2021: Differential regulation of endoplasmic reticulum stress-induced autophagy and apoptosis in two strains of gibel carp (*Carassius gibelio*) exposed to acute waterborne cadmium. *Aquat. Toxicol.* 231: 105721.
- Limbaugh N., Romano N., Egnew N. et al. 2021: Coping strategies in response to different levels of elevated water hardness in channel catfish (*Ictalurus punctatus*): insight into ion-regulatory



- and histopathological modulations. *Comp. Biochem. Physiol. A Mol. Integr. Physiol.* 260: 111040.
- Makarenko A., Mushtruk M., Rudyk-Leuska N. et al. 2022: Investigation of internal organs and additive tissue of hybrid hypophthalmichthys (*Hypophthalmichthys* spp.) as a promising raw material for the production of dietary nutritional products. *Potr. S. J. F. Sci.* 16: 411–430.
- Manrique W.G., Pereira Figueiredo M.A., Charlie-Silva I. et al. 2019: Spleen melanomacrophage centers response of Nile tilapia during *Aeromonas hydrophila* and *Mycobacterium marinum* infections. *Fish Shellfish Immunol.* 95: 514–518.
- Marancik D.P., Leeds T.D. & Wiens G.D. 2014: Histopathologic changes in disease-resistant-line and disease-susceptible-line juvenile rainbow trout experimentally infected with *Flavobacterium psychrophilum*. *J. Aquat. Anim. Health* 26: 181–189.
- Menon S.V., Kumar A., Middha S.K. et al. 2023: Water physicochemical factors and oxidative stress physiology in fish, a review. *Front. Environ. Sci.* 11: 1240813.
- Mikula P., Modra H., Nemethova D. et al. 2008: Effects of subchronic exposure to LASSO MTX (alachlor 42% W/V) on hematological indices and histology of the common carp, *Cyprinus carpio* L. *Bull. Environ. Contam. Toxicol.* 81: 475–479.
- Mitsoura A., Kagalogu I., Papaioannou N. et al. 2013: The presence of microcystins in fish *Cyprinus carpio* tissues: a histopathological study. *Int. Aquat. Res.* 5: 8.
- Mokhtar D.M. 2018: Cellular and stromal elements organization in the liver of grass carp, *Ctenopharyngodon idella* (Cypriniformes: Cyprinidae). *Micron* 112: 1–14.
- Montero D., Blazer V.S., Socorro J. et al. 1999: Dietary and culture influences on macrophage aggregate parameters in gilthead seabream (*Sparus aurata*) juveniles. *Aquaculture* 179: 523–534.
- Myers R. 2024: Special stain techniques for the evaluation of mucins. <http://www.leicabiosystems.com/pathologyleaders/special-stain-techniques-for-the-evaluation-of-mucins/>
- Mæland A., Rønnestad I., Fyhn H.J. et al. 2000: Water-soluble vitamins in natural plankton (copepods) during two consecutive spring blooms compared to vitamins in *Artemia franciscana* nauplii and metanauplii. *Mar. Biol.* 136: 765–772.
- Naguib M., Mahmoud U.M., Mekawy I.A. et al. 2020: Hepatotoxic effects of silver nanoparticles on *Clarias gariepinus*; biochemical, histopathological, and histochemical studies. *Toxicol. Rep.* 7: 133–141.
- Noyes A.D., Grizzle J.M. & Plumb J.A. 1991: Hematology and histopathology of an idiopathic anemia of channel catfish. *J. Aquat. Anim. Health* 3: 161–167.
- Okas A., Kowalczyk J., Stein R. et al. 2001: Hypoxic hepatitis related to profound anemia: how low can you go? *Am. J. Gastroenterol.* 96: 3445–3447.
- Passantino L., Corriero A., Pousis C. et al. 2024: Hepatic melanomacrophage centers in the arctic cultured fish *Cyclopterus lumpus* are not indicative of its health state. *Aquaculture* 581: 740417.
- Peters N., Köhler A. & Kranz H. 1987: Liver pathology in fishes from the Lower Elbe as a consequence of pollution. *Dis. Aquat. Org.* 2: 87–97.
- Press C.M. & Evensen Ø. 1999: The morphology of the immune system in teleost fishes. *Fish Shellfish Immunol.* 9: 309–318.
- Pronina S.V., Batueva M.D.D. & Pronin N.M. 2014: Characteristics of melanomacrophage centers in the liver and spleen of the roach *Rutilus rutilus* (Cypriniformes: Cyprinidae) in lake Kotokel during the Haff disease outbreak. *J. Ichthyol.* 54: 104–110.
- Rebok K., Jordanova M. & Tavciovaska-Vasileva I. 2011: Spleen histology in the female Ohrid trout, *Salmo letnica* (Kar.) (Teleostei, Salmonidae) during the reproductive cycle. *Arch. Biol. Sci.* 63: 1023–1030.
- Renaut S. & Bernatchez L. 2011: Transcriptome-wide signature of hybrid breakdown associated with intrinsic reproductive isolation in lake whitefish species pairs (*Coregonus* spp. Salmonidae). *Heredity* 106: 1003–1011.
- Renaut S., Nolte A.W. & Bernatchez L. 2009: Gene expression divergence and hybrid misexpression between lake whitefish species pairs (*Coregonus* spp. Salmonidae). *Mol. Biol. Evol.* 26: 925–936.
- Roberts R.J. & Rodger H.D. 2012: The pathophysiology and systematic pathology of teleosts. In: Roberts R.J. (ed.), *Fish pathology*. John Wiley & Sons Ltd., London, UK: 62–143.
- Rocha E., Monteiro R.A. & Pereira C.A. 1994: The liver of the brown trout, *Salmo trutta* fario: a light and electron microscope study. *J. Anat.* 185: 241–249.
- Rosenthal K.D., Brown D.A., Cross J.N. et al. 1984: Histological condition of fish livers. *SCCWRP Biennial Report 1983-1984*: 229–245.
- Roy George K., Malini N.A. & Rajasree D. 2015: Effects of acclimation on the haematological indices of different groups of fresh water teleosts. *J. Nat. Appl. Sci.* 7: 5–9.



- Ruiz M.L., Owatari M.S., Yamashita M.M. et al. 2020: Histological effects on the kidney, spleen, and liver of Nile tilapia *Oreochromis niloticus* fed different concentrations of probiotic *Lactobacillus plantarum*. *Trop. Anim. Health Prod.* 52: 167–176.
- Ruiz-Ramírez J.A., Ramírez-Ayala E., Tintos-Gómez A. et al. 2019: Hepatocellular steatosis as a response to nutritional stressors in *Lutjanus guttatus* (Steindachner, 1869) grown in floating cages: a case study. *Lat. Am. J. Aquat. Res.* 47: 709–715.
- Sales C.F., Silva R.F., Amaral M.G.C. et al. 2017: Comparative histology in the liver and spleen of three species of freshwater teleost. *Neotrop. Ichthyol.* 15: e160041.
- Sayed R.K.A., Zaccane G., Capillo G. et al. 2022: Structural and functional aspects of the spleen in molly fish *Poecilia sphenops* (Valenciennes, 1846): synergistic interactions of stem cells, neurons, and immune cells. *Biology* 11: 779.
- Souza V.L., Lunardi L.O., Vasques L.H. et al. 2001: Morphometric alterations in hepatocytes and ultrastructural distribution of liver glycogen in pacu (*Piaractus mesopotamicus* Holmberg, 1887) during food restriction and refeeding. *Braz. J. Morphol. Sci.* 18: 15–20.
- Speare D.J. 2000: Liver diseases of tropical fish. *Semin. Avian Exot. Pet Med.* 9: 174–178.
- Spengler E. & Fontana R.J. 2018: Acute liver failure. In: Friedman L.S. & Martin P. (eds.), *Handbook of liver disease*, 4th ed. Elsevier, Amsterdam, Netherlands: 18–33.
- Steinel N.C. & Bolnick D.I. 2017: Melanomacrophage centers as a histological indicator of immune function in fish and other poikilotherms. *Front. Immunol.* 8: 827.
- Stelkens R.B., Schmid C. & Seehausen O. 2015: Hybrid breakdown in cichlid fish. *PLOS ONE* 10: e0127207.
- Sun Y., Guo C.-Y., Wang D.-D. et al. 2016: Transcriptome analysis reveals the molecular mechanisms underlying growth superiority in a novel grouper hybrid (*Epinephelus fuscogutatus* × *E. lanceolatus*). *BMC Genet.* 17: 24.
- Swain S., Sawant P.B., Chadha N.K. et al. 2020: Significance of water pH and hardness on fish biological processes: a review. *Int. J. Chem. Stud.* 8: 330–337.
- Šimková A., Cíváňová K. & Vetešník L. 2022: Heterosis versus breakdown in fish hybrids revealed by one-parental species-associated viral infection. *Aquaculture* 546: 737406.
- Šimková A., Dávidová M., Papoušek I. et al. 2013: Does interspecies hybridization affect the host specificity of parasites in cyprinid fish? *Parasit. Vectors* 6: 95.
- Šimková A., Janáč M., Hyršl P. et al. 2021: Vigour-related traits and immunity in hybrids of evolutionary divergent cyprinoid species: advantages of hybrid heterosis? *J. Fish Biol.* 98: 1155–1171.
- Šimková A., Křížová K.C., Voříšková K. et al. 2024: Heterosis versus breakdown in cyprinid hybrids associated with SVCV infection revealed by transcriptome profile analysis of head kidney. *Aquaculture* 578: 740083.
- Šimková A., Vojtek L., Halačka K. et al. 2015: The effect of hybridization on fish physiology, immunity and blood biochemistry: a case study in hybridizing *Cyprinus carpio* and *Carassius gibelio* (Cyprinidae). *Aquaculture* 435: 381–389.
- Tanuma Y. 1980: Electron microscope observations on the intrahepatocytic bile canalicules and sequent bile ductules in the crucian, *Carassius carassius*. *Arch. Histol. Jpn.* 43: 1–21.
- Tichopád T., Vetešník L., Šimková A. et al. 2020: Spermatozoa morphology and reproductive potential in F1 hybrids of common carp (*Cyprinus carpio*) and gibel carp (*Carassius gibelio*). *Aquaculture* 521: 735092.
- Torbenson M., Kakar S. & Washington K. 2022: Core pathology patterns in medical liver specimens. In: Torbenson M., Kakar S. & Washington K. (eds.), *Non-neoplastic diseases of the liver. American Registry of Pathology, Rockville, USA*: 1–25.
- Uyisenga A., Liang H., Ren M. et al. 2023: The effects of replacing fish meal with enzymatic soybean meal on the growth performance, whole-body composition, and health of juvenile gibel carp (*Carassius auratus gibelio*). *Fishes* 8: 423.
- Valigurová A. & Koudela B. 2008: Morphological analysis of the cellular interactions between the eugregarine *Gregarina garnhami* (Apicomplexa) and the epithelium of its host, the desert locust *Schistocerca gregaria*. *Eur. J. Protistol.* 44: 197–207.
- Vetešník L., Pojezdal L., Reschová S. et al. 2024: Specific anti-SVCV antibodies in hybrids of common carp (*Cyprinus carpio*) and gibel carp (*Carassius gibelio*) reflect heterosis advantage and genetic breakdown. *Aquaculture* 593: 741320.
- Witeska M. 2015: Anemia in teleost fishes. *Bull. Eur. Assoc. Fish Pathol.* 35: 148–160.
- Wolf J.C. & Wheeler J.R. 2018: A critical review of histopathological findings associated with

- endocrine and non-endocrine hepatic toxicity in fish models. *Aquat. Toxicol.* 197: 60–78.
- Wolf J.C. & Wolfe M.J. 2005: A brief overview of nonneoplastic hepatic toxicity in fish. *Toxicol. Pathol.* 33: 75–85.
- Wolke R.E. 1992: Piscine macrophage aggregates: a review. *Annu. Rev. Fish Dis.* 2: 91–108.
- Yang S., Luo J., Long Y. et al. 2019: Mixed diets reduce the oxidative stress of common carp (*Cyprinus carpio*): based on microRNA sequencing. *Front. Physiol.* 10: 631.
- Yang L., Zhao M., Liu M. et al. 2023: Effects of genistein on lipid metabolism, antioxidant activity, and immunity of common carp (*Cyprinus carpio* L.) fed with high-carbohydrate and high-fat diets. *Aquac. Nutr.* 2023: 9555855.
- Yao Y., Lin J., Yang P. et al. 2012: Fine structure, enzyme histochemistry, and immunohistochemistry of liver in zebrafish. *Anat. Rec.* 295: 567–576.
- Zapata A.G. 2024: The fish spleen. *Fish Shellfish Immunol.* 144: 109280.
- Zhang X.-J., Zhou L., Lu W.-J. et al. 2021: Comparative transcriptomic analysis reveals an association of gibel carp fatty liver with ferroptosis pathway. *BMC Genomics* 22: 328.
- Zhao Y., Weng M., Zhang Q. et al. 2021: Transcriptomics analysis of the infected tissue of gibel carp (*Carassius auratus gibelio*) with liver myxobolosis infers the underlying defense mechanisms from the perspective of immune-metabolic interactions. *Aquaculture* 542: 736867.
- Zhong L., Liu H., Zhang H. et al. 2022: High starch in diet leads to disruption of hepatic glycogen metabolism and liver fibrosis in largemouth bass (*Micropterus salmoides*), which is mediated by the PI3K/Akt signaling pathway. *Front. Physiol.* 13: 880513.
- Zhou W., Liang H. & Zhang X. 2012: Erythrocyte damage of crucian carp (*Carassius auratus*) caused by microcystin-LR: in vitro study. *Fish Physiol. Biochem.* 38: 849–858.

List of abbreviations

AB – Alcian blue
 BF-LM – bright-field light microscopy
 BC CaF1 – backcross *C. gibelio* × F1 hybrid
 BC CyF1 – backcross *C. carpio* × F1 hybrid
 BC F1Ca – backcross F1 hybrid × *C. gibelio*
 BC F1Cy – backcross F1 hybrid × *C. carpio*
 CaCa – pure *C. gibelio*
 CyCy – pure *C. carpio*
 F1 CaCy – F1 *C. gibelio* × *C. carpio*
 F1 CyCa – F1 *C. carpio* × *C. gibelio*
 F2 – F2 generation
 HE – haematoxylin-eosin
 HIS – hepatosomatic index
 MMCs – melanomacrophage centers
 MT – Masson's trichrome
 PAS – Periodic Acid-Schiff
 RER – rough endoplasmic reticulum
 SSI – spleen-somatic index
 TEM – transmission electron microscopy

Supplementary online material

Fig. S1. Comparison of splenic melanomacrophage centres in experimental and wild control fish. (a-b) Pure *Cyprinus carpio*. (a) General view of the splenic parenchyma of experimental fish with few MMCs containing the brown pigment, compared to (b) the spleen of wild common carp exhibiting the abundant and much larger light-pigmented MMCs. (c-d) Pure *Carassius gibelio*. (c) General view of the splenic pachynema of experimental fish with numerous MMCs compared to (d) the spleen of wild gibel carp with less frequent MMCs containing lighter pigment. (e-f) F1 *C. gibelio* × *C. carpio*. (e) General view of the splenic parenchyma of experimental fish



with abundant MMCs varying in size and containing the dark brown pigment, compared to (f) the spleen of wild F1 hybrids showing significantly higher variability in the number and size of MMCs. While one individual showed frequent and variously sized MMCs with dark brown pigment (i), another had only a few medium-sized MMCs with lighter pigment (ii). (a-c): paraffine sections stained with haematoxylin-eosin, BF-LM. f – fibrosis; mc – melanomacrophage centres; n – necrosis (<https://www.ivb.cz/wp-content/uploads/JVB-vol.-74-2025-Valigurova-A.-et-al.-Fig.-S1-1.pdf>).

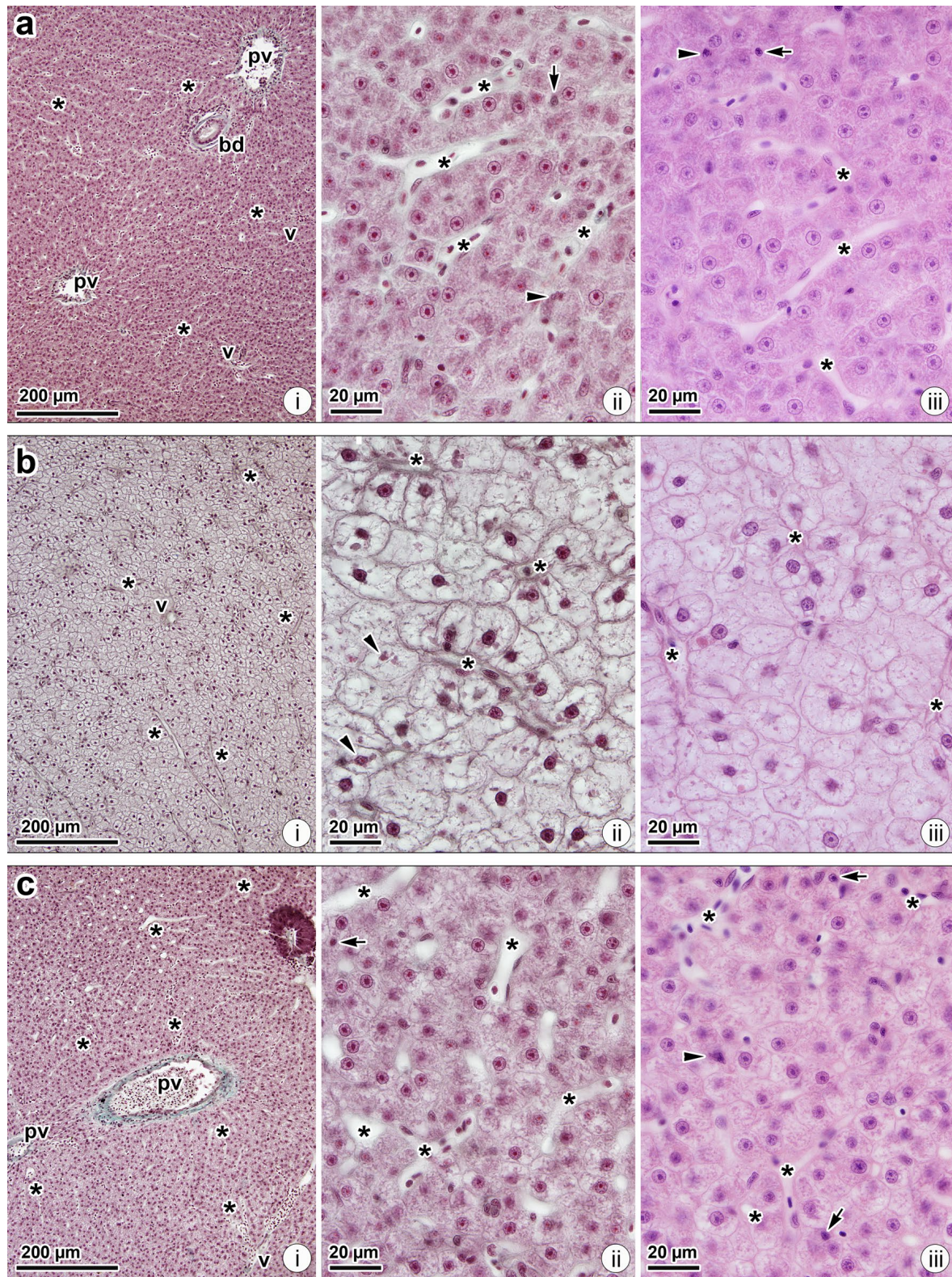


Fig. 1. Liver architecture in pure *Cyprinus carpio*, pure *Carassius gibelio* and F1 generation with *C. gibelio* mtDNA. (a) Pure *C. carpio*. General view (i) of the liver parenchyma. Detailed views (ii, iii) of the parenchyma showing hepatocytes with a slightly outlined polyhedral shape and with confluent borders. Note the densely granulated hepatocyte cytoplasm with a high affinity for plasma dyes. (b) Pure *C. gibelio*. General view (i) of the liver parenchyma. Detailed views (ii, iii) of the parenchyma with hypertrophic hepatocytes. Note the wavy plasma membrane lining the more or less polyhedral hepatocytes, the colourless cytoplasm with few granules, and the irregularly shaped, highly condensed nuclei. (c) F1 *C. gibelio* × *C. carpio*. General view (i) of the liver parenchyma. Detailed views (ii, iii) of the parenchyma revealing that hepatocytes with granular, strongly eosinophilic cytoplasm alternate with hepatocytes with vacuolated cytoplasm. Note the distinct plasma membrane lining the hepatocytes. Applies to (a-c): paraffine sections stained with Masson's trichrome (i, ii) or haematoxylin-eosin (iii), BF-LM. bd – bile duct; black arrow – pycnotic hepatocyte; black arrowhead – karyorrhectic hepatocyte; black asterisk – sinusoid(s); pv – portal vein; v – central vein.

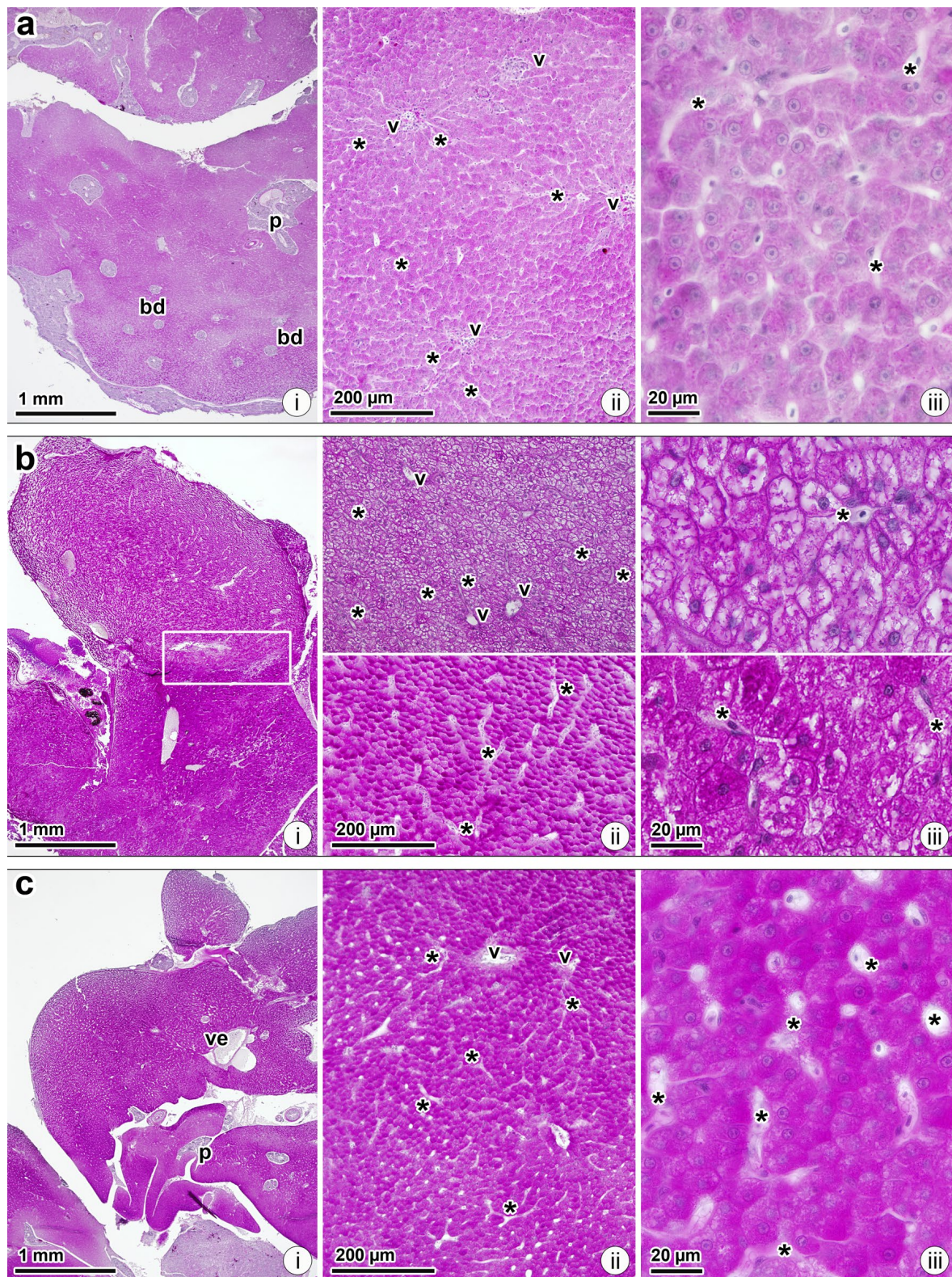


Fig. 2. Liver glycogen storage in pure *Cyprinus carpio*, pure *Carassius gibelio* and F1 generation with *C. gibelio* mtDNA. (a) Pure *C. carpio*. General view (i) and higher magnification (ii) of liver sections with a low glycogen load. Note the hepatocyte cytoplasm with a granular pattern (iii). (b) Pure *C. gibelio*. General view (i) and higher magnification (ii) of liver sections with a high glycogen content. Note the upper part of the tissue (i) with hepatocytes with glycogen accumulating at their periphery and in rays radiating from the nucleus (ii, iii – top micrographs), and the lower tissue area (i) with irregularly distributed glycogen of higher concentration giving the hepatocytes a cup-like appearance (ii, iii – bottom micrographs). (c) F1 *C. gibelio* × *C. carpio*. General view (i) and higher magnification (ii) of liver sections with a high glycogen load regularly distributed throughout the tissue, where the peripheral tissue shows less intense staining than its central area. The high glycogen load in the cytoplasm led to very intense staining overlapping the boundaries of individual hepatocytes (iii). Applies to (a-c): paraffine sections stained with Alcian Blue-Periodic Acid-Schiff, BF-LM. bd – bile duct; black asterisk – sinusoid(s); p – pancreatic tissue; v – central vein; ve – blood vessel; white rectangle – necrotic area.

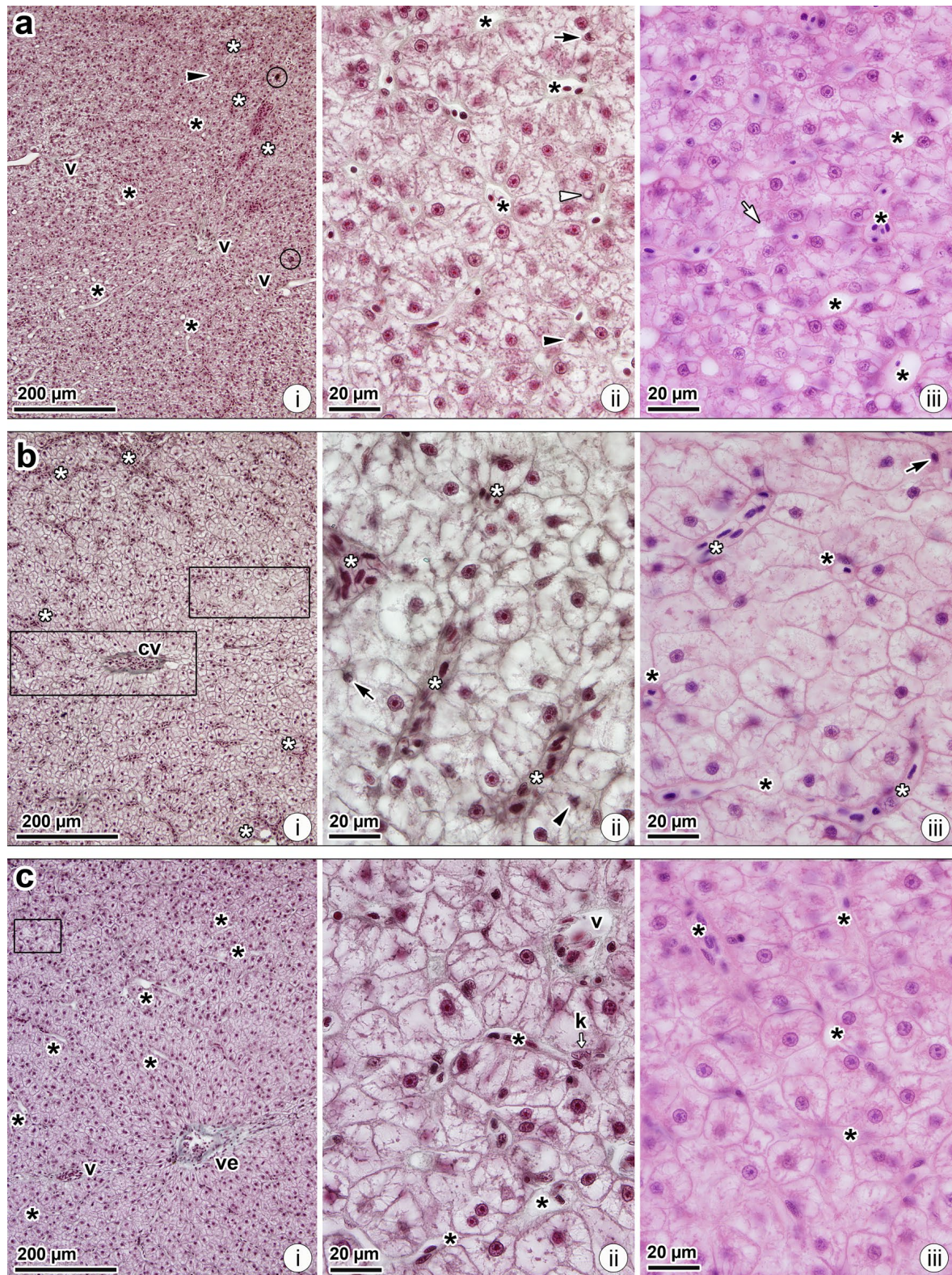


Fig. 3. Liver architecture in F1 generation with *Cyprinus carpio* mtDNA and maternal backcrosses. (a) F1 *C. carpio* × *C. gibelio*. General view (i) of the liver parenchyma. Detailed views (ii, iii) of the parenchyma with polyhedral hepatocytes clearly demarcated by their plasma membranes. Note the less granulated cytoplasm of hepatocytes with lower affinity for plasma dyes. (b) Backcross *C. gibelio* × F1 hybrid. General view (i) of the liver parenchyma. Detailed views (ii, iii) of the parenchyma with hypertrophic hepatocytes. Note that the hepatocytes of various sizes have almost colourless cytoplasm without granules and condensed nuclei. (c) Backcross F1 hybrid × *C. gibelio*. General view (i) of the liver parenchyma. Detailed views (ii, iii) of the parenchyma with hypertrophic hepatocytes clearly demarcated by their wavy plasma membranes. The hepatocyte cytoplasm shows mild granulation surrounding a condensed nucleus with irregular nucleolus. Applies to (a-c): paraffine sections stained with Masson's trichrome (i, ii) or haematoxylin-eosin (iii), BF-LM. black arrow – pycnotic hepatocyte; black arrowhead – karyorrhectic hepatocyte; black asterisk – sinusoid(s); black circle – MMCs; black rectangle – necrotic area; cv – congested vein; k – Kupffer cell; v – central vein; ve – blood vessel; white asterisk – congested sinusoid(s); white arrowhead – nuclear vacuolisation; white arrow – single cell necrosis.

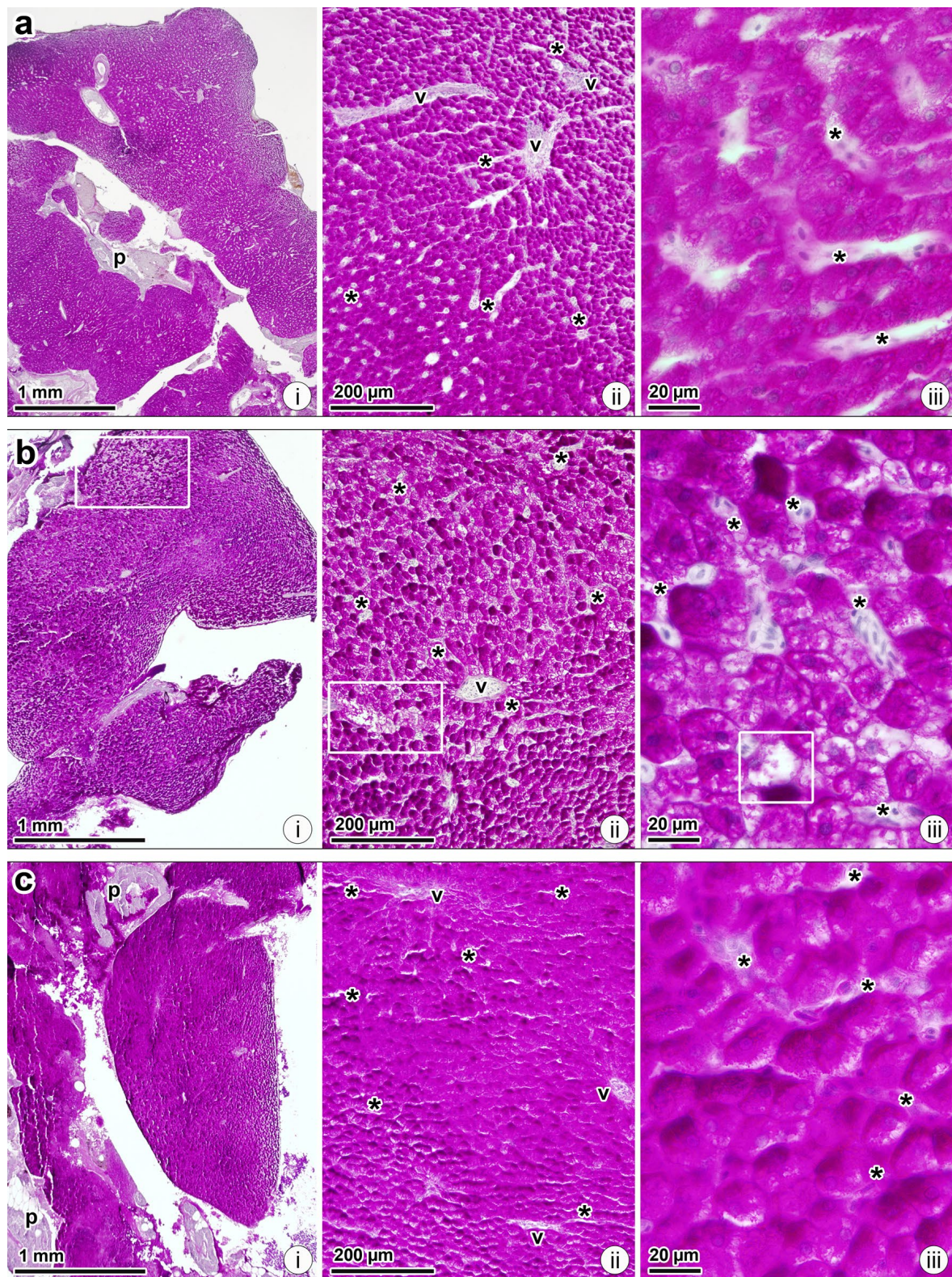


Fig. 4. Liver glycogen storage in F1 generation with *Cyprinus carpio* mtDNA and maternal backcrosses. (a) F1 *C. carpio* × *C. gibelio*. General view (i) and higher magnification (ii) of liver sections with very abundant glycogen, the central tissue being more intensively stained than its periphery. Detailed view revealing extremely high glycogen load in hepatocytes where staining overlapped their boundaries (iii). (b) Backcross *C. gibelio* × F1 hybrid. General view (i) and higher magnification (ii) of liver sections with very abundant glycogen regularly distributed through the tissue. Hepatocytes either have the glycogen accumulated at their periphery and in rays radiating from the nucleus, or the very intense PAS staining evenly covered the entire cell (iii). (c) Backcross F1 hybrid × *C. gibelio*. General view (i) and higher magnification (ii) of liver sections revealing the highest glycogen load among all fish lines. The very intense PAS staining completely covers the hepatocytes (iii). Applies to (a-c): paraffine sections stained with Alcian Blue-Periodic Acid-Schiff, BF-LM. black asterisk – sinusoid(s); p – pancreatic tissue; v – central vein; white rectangle – necrotic area.

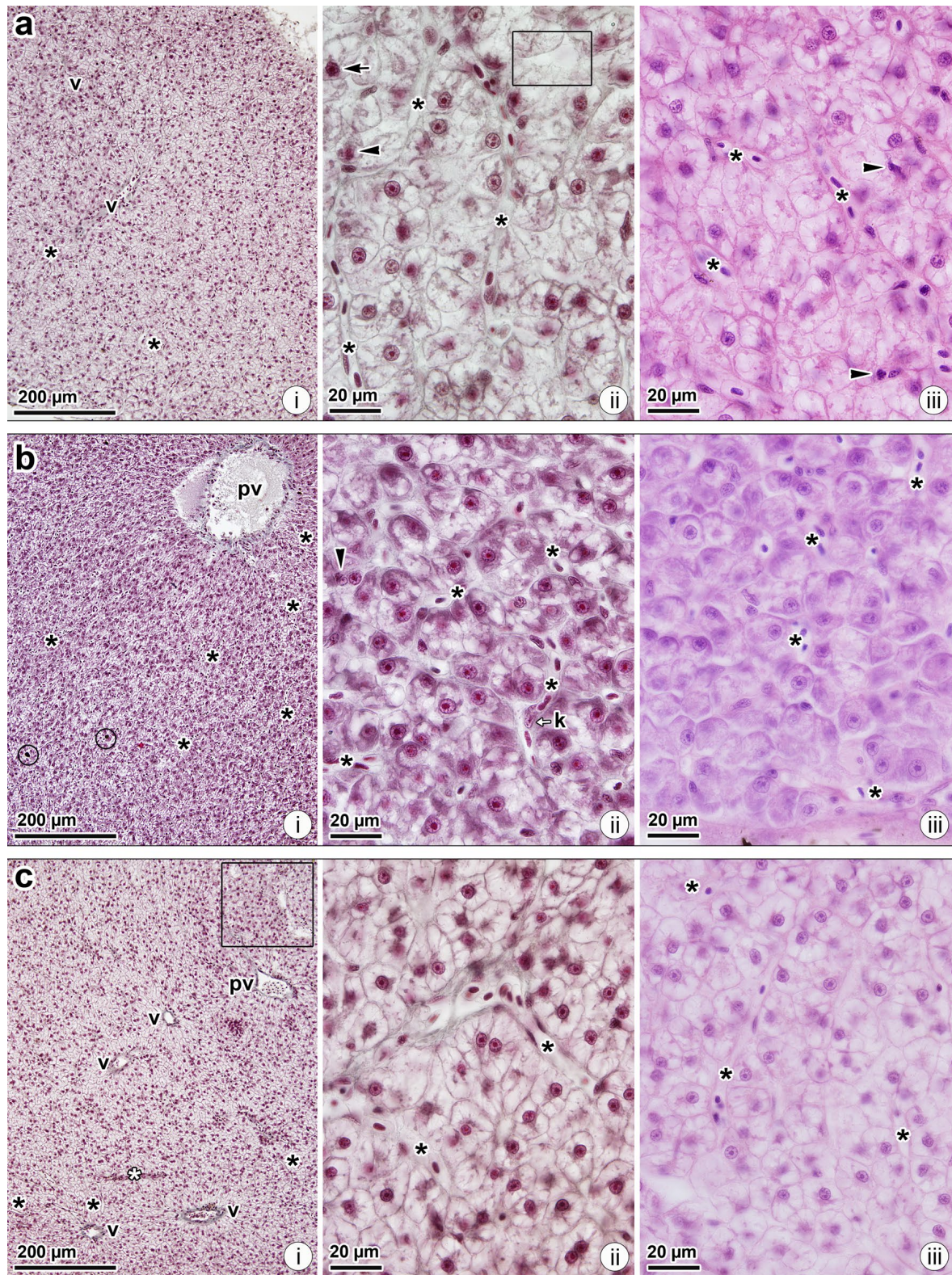


Fig. 5. Liver architecture in paternal backcrosses and F2 generation. (a) Backcross *C. carpio* × F1 hybrid. General view (i) of the liver parenchyma. Detailed views (ii, iii) of the parenchyma consisting of hypertrophic hepatocytes varying in shape and size, with almost colourless cytoplasm lacking granulation. Note the distinct but discontinuous demarcation of hepatocytes by their plasma membranes. (b) Backcross F1 hybrid × *C. carpio*. General view (i) of the liver parenchyma. Detailed views (ii, iii) of the parenchyma consisting of hepatocytes with cytoplasm divided into granular (basophilic) and vacuolated regions. Note the large nuclei and condensed nucleoli. (c) F2 generation. General view (i) of the liver parenchyma. Detailed views (ii, iii) of the parenchyma with hypertrophic polyhedral hepatocytes. Note the distinct demarcation of the hepatocytes by their slightly wavy plasma membranes and the condensed nuclei. Applies to (a-c): paraffine sections stained with Masson's trichrome (i, ii) or haematoxylin-eosin (iii), BF-LM. black arrow – pycnotic hepatocyte; black arrowhead – karyorrhectic hepatocyte; black asterisk – sinusoid(s); black circle – MMCs; black rectangle – necrotic area; k – Kupffer cell; pv – portal vein; v – central vein; white asterisk – congested sinusoid(s).

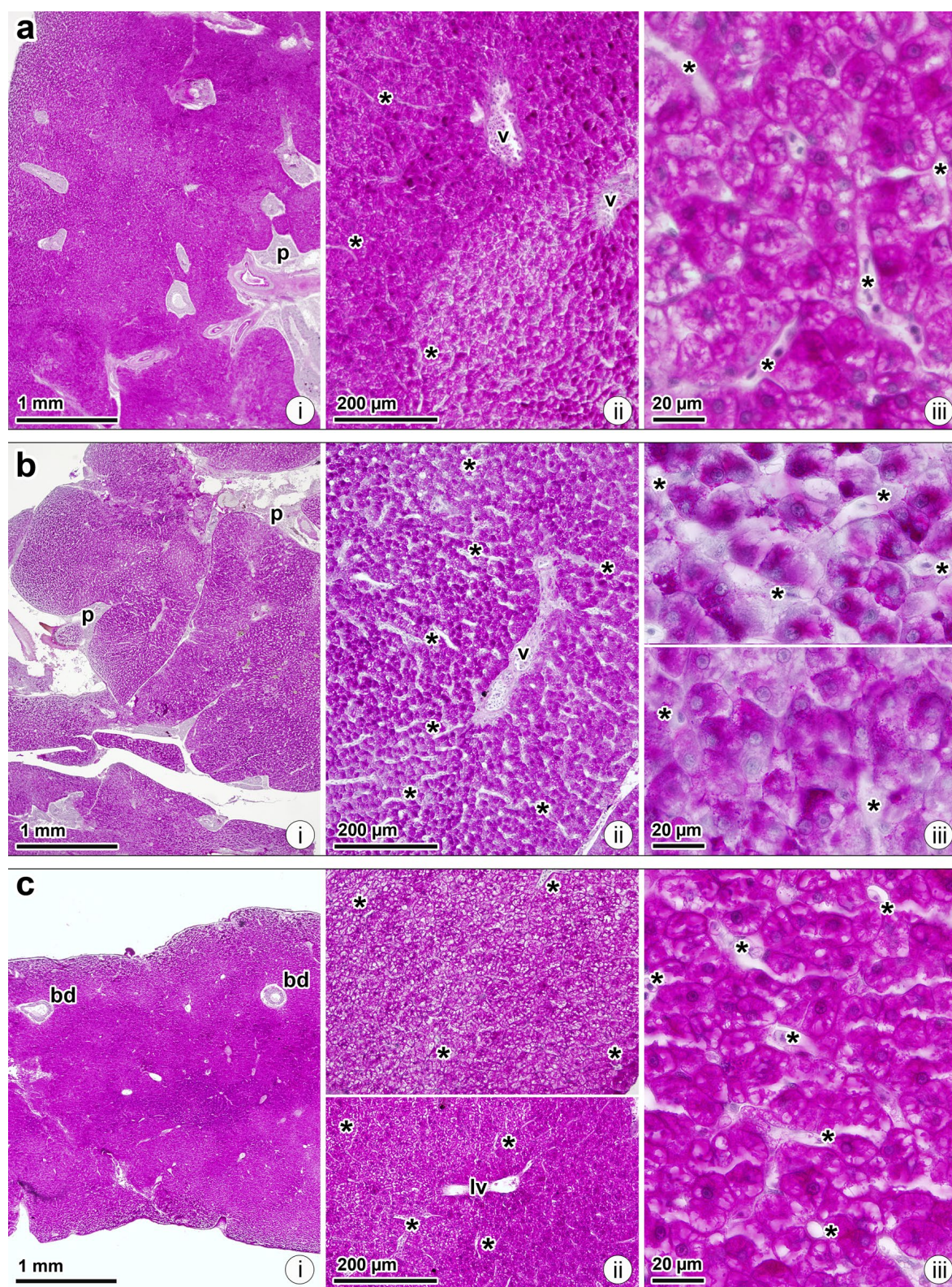


Fig. 6. Liver glycogen storage in paternal backcrosses and F2 generation. (a) Backcross *C. carpio* × F1 hybrid. General view (i) and higher magnification (ii) of liver sections with abundant glycogen irregularly distributed through the tissue. The glycogen is either concentrated at the hepatocyte periphery and in radial protrusions around the nucleus, or the intense PAS staining uniformly covers almost the entire cell. (b) Backcross F1 hybrid × *C. carpio*. General view (i) and higher magnification (ii) of liver sections with a moderate glycogen load irregularly distributed throughout the tissue. The uneven distribution of glycogen is well visible at higher magnification (iii – top micrograph vs. bottom micrograph). The cytoplasm of hepatocytes shows unstained areas alternating with intensely stained ones (iii). (c) F2 generation. General view (i) and higher magnification (ii) of liver sections with very abundant glycogen. The peripheral tissue (ii – top micrograph) shows less intense PAS staining than the central region (ii – bottom micrograph). Most hepatocytes have glycogen accumulated at the periphery and radially around the nucleus, while some show intense staining covering the entire cell (iii). Applies to (a-c): paraffine sections stained with Alcian Blue-Periodic Acid-Schiff, BF-LM. bd – bile duct; black asterisk – sinusoid(s); lv – lymphatic vessel; p – pancreatic tissue; v – central vein.

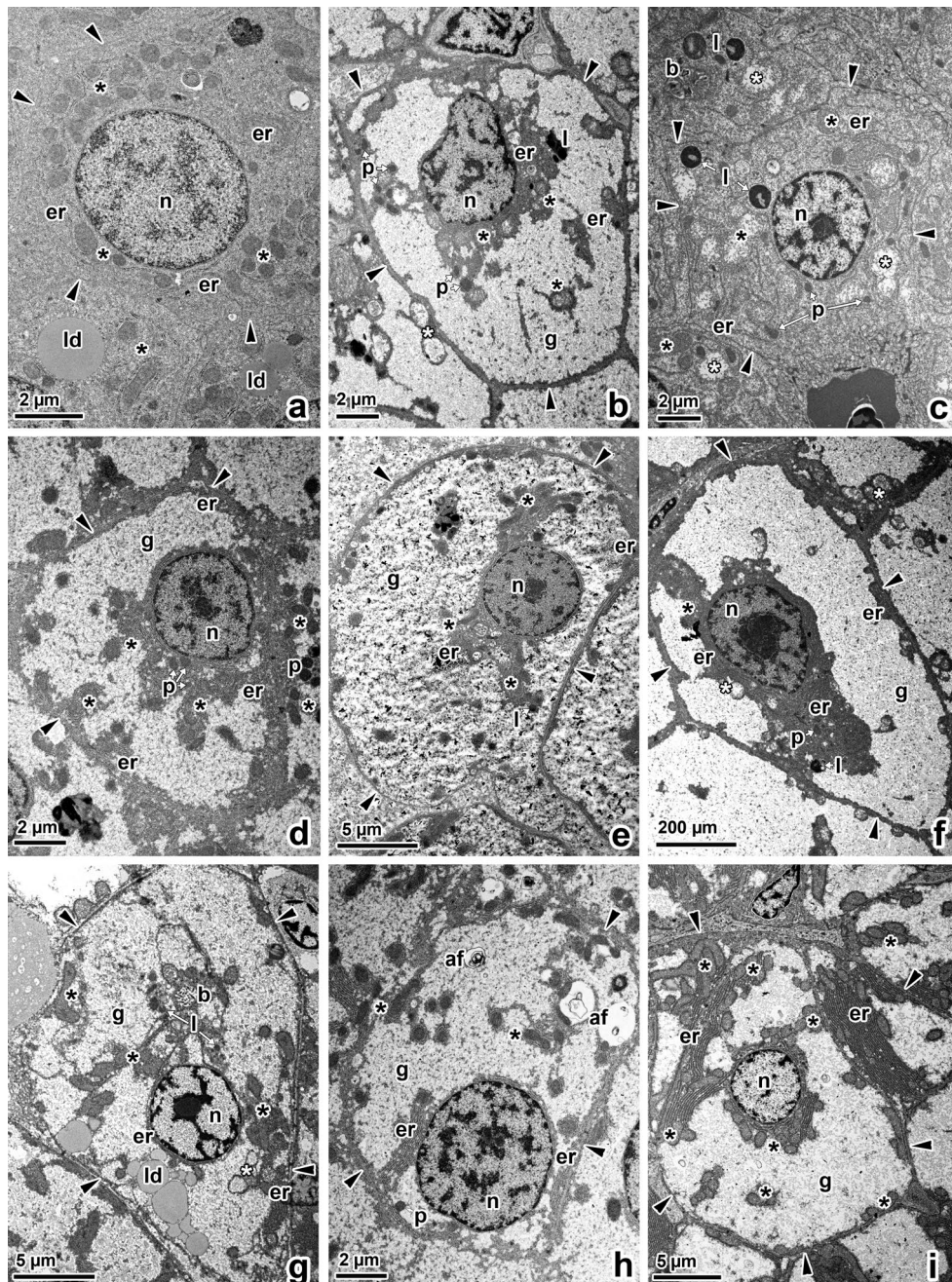


Fig. 7. Subcellular organisation of hepatocytes in all fish lines. (a) Pure *C. carpio*. The homogeneously granulated cytoplasm of the roundish hepatocyte is packed with several RER lamellae and abundant mitochondria surrounding the large round nucleus. (b) Pure *C. gibelio*. The cytoplasm of the polyhedral hepatocyte is packed with glycogen particles, large mitochondria, and RER. The RER lamellae are concentrated around the irregular nucleus and beneath the plasma membrane. (c) F1 *C. gibelio* × *C. carpio*. The almost homogeneously granulated cytoplasm of the roundish hepatocyte is packed with numerous swollen mitochondria, RER and a small nucleus. Note the dense autophagosomes with lamellar contents. (d) F1 *C. carpio* × *C. gibelio*. The cytoplasm of the polyhedral hepatocyte is filled with abundant glycogen particles, RER and abundant mitochondria. The RER lamellae are accumulated around the roundish nucleus and form an irregularly thick layer beneath the plasma membrane. (e) Backcross *C. gibelio* × F1 hybrid. The cytoplasm of the polyhedral hepatocyte is packed with glycogen particles, few mitochondria, RER, and a round nucleus. The plasma membrane is underlain by the RER lamellae. (f) Backcross F1 hybrid × *C. gibelio*. The electron-lucent cytoplasm of the polyhedral hepatocyte is packed with glycogen particles, RER and a few small mitochondria. While most RER lamellae are concentrated around the irregularly shaped nucleus, a few form a thin layer lining the cytoplasmic face of the plasma membrane. (g) Backcross *C. carpio* × F1 hybrid. The cytoplasm of the polyhedral hepatocyte is packed with abundant glycogen particles, several lipid droplets, numerous mitochondria, a round nucleus, and a small amount of RER. (h) Backcross F1 hybrid × *C. carpio*. The hepatocyte cytoplasm contains a large, slightly oval nucleus, abundant glycogen particles, and numerous mitochondria surrounded by several RER lamellae. The RER also forms an irregular layer lining the cytoplasmic face of the plasma membrane. (i) F2 generation. The cytoplasm of the polyhedral hepatocyte is packed with abundant glycogen particles, numerous mitochondria and a massive RER. The RER lamellae are accumulated around the round nucleus and on one side of the hepatocyte, while several lamellae surround the mitochondria and line the cytoplasmic face of the plasma membrane. Applies to (a-i): TEM. af – autophagosome; b – bile canaliculus; black arrowheads – hepatocyte plasma membrane; black asterisk – mitochondria; er – rough endoplasmic reticulum; g – glycogen; l – lysosome; ld – lipid droplet; p – peroxisome; n – hepatocyte nucleus; white asterisk – swollen mitochondria.

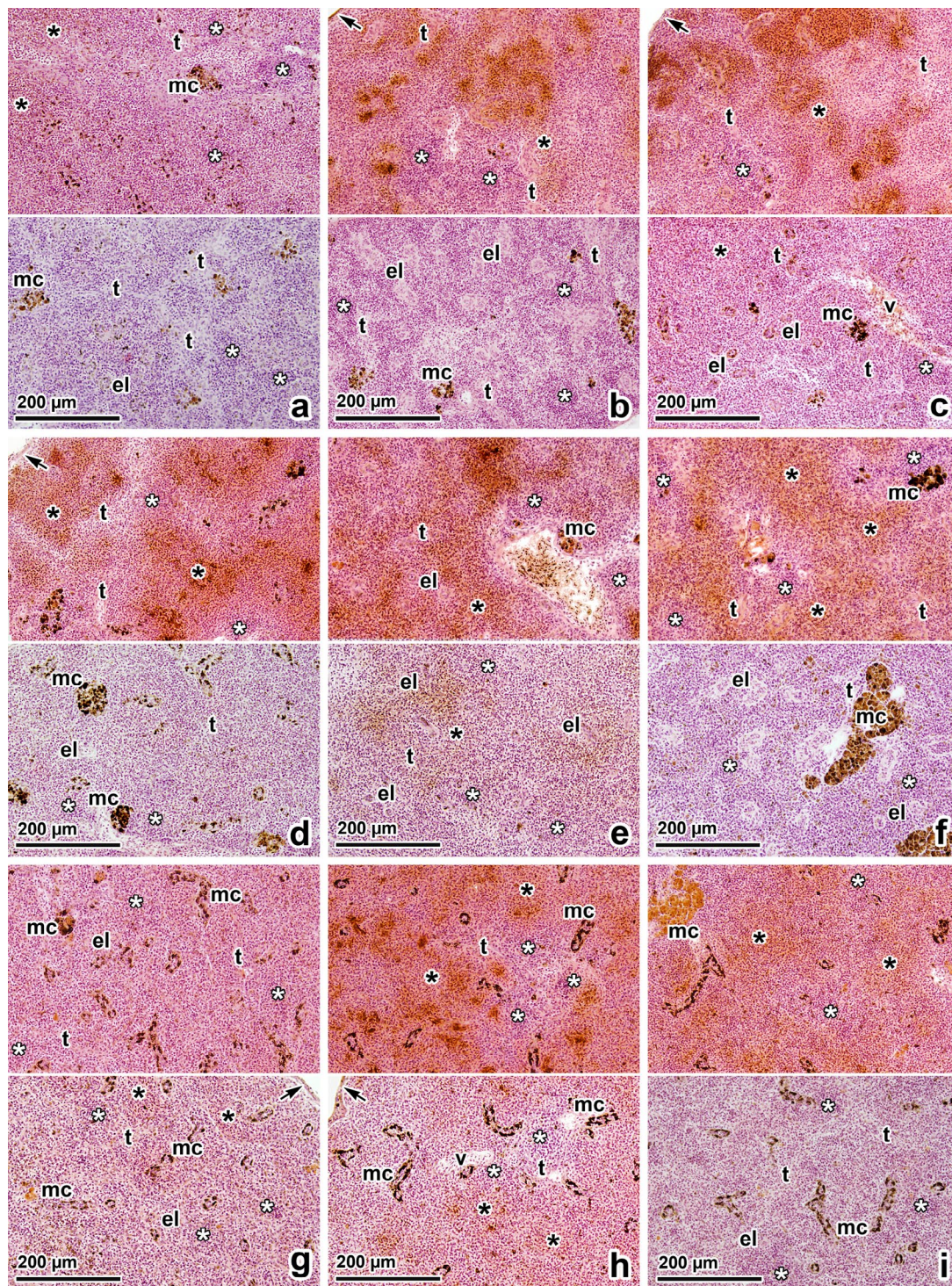


Fig. 8. General view of the splenic parenchyma in all fish lines. (a) Pure *C. carpio*. Splenic parenchyma with normal appearance (lower micrograph), and parenchyma with increased accumulation of erythrocytes (upper micrograph). (b) Pure *C. gibelio*. Splenic parenchyma depleted of erythrocytes (lower micrograph), and parenchyma showing severe haemolysis and focal deposition of hematogenous pigments (upper micrograph). (c) F1 *C. gibelio* × *C. carpio*. Normal-appearing splenic parenchyma (lower micrograph) and parenchyma with severe haemolysis and foci of deposited pigments (upper micrograph). (d) F1 *C. carpio* × *C. gibelio*. Normal-appearing splenic parenchyma containing MMCs of various sizes (lower micrograph) and parenchyma with severe haemolysis and pigment deposition (upper micrograph). (e) Backcross *C. gibelio* × F1 hybrid. Splenic parenchyma showing mild haemolysis detectable by the deposited brown pigment (lower micrograph) and parenchyma with moderate to severe haemolysis and foci of deposited pigments (upper micrograph). (f) Backcross F1 hybrid × *C. gibelio*. Splenic parenchyma is depleted of erythrocytes and contains large MMCs (lower micrograph). Parenchyma shows moderate to severe haemolysis and pigment deposition (upper micrograph). (g) Backcross *C. carpio* × F1 hybrid. Splenic parenchyma with almost normal appearance (lower micrograph) and parenchyma showing moderate diffuse haemolysis (upper micrograph). (h) Backcross F1 hybrid × *C. carpio*. Splenic parenchyma showing very mild haemolysis (lower micrograph) and parenchyma with severe haemolysis and foci of deposited pigments (upper micrograph). (i) F2 generation. Normal-appearing splenic parenchyma (lower micrograph) and parenchyma showing moderate to severe diffuse haemolysis with pigment deposition (upper micrograph). Applies to (a-i): paraffine sections stained with haematoxylin-eosin, BF-LM. black arrow – capsule; black asterisks – red pulp; el – ellipsoid; mc – melanomacrophage centres (MMCs); v – vein; t – trabeculae; white asterisk – white pulp.

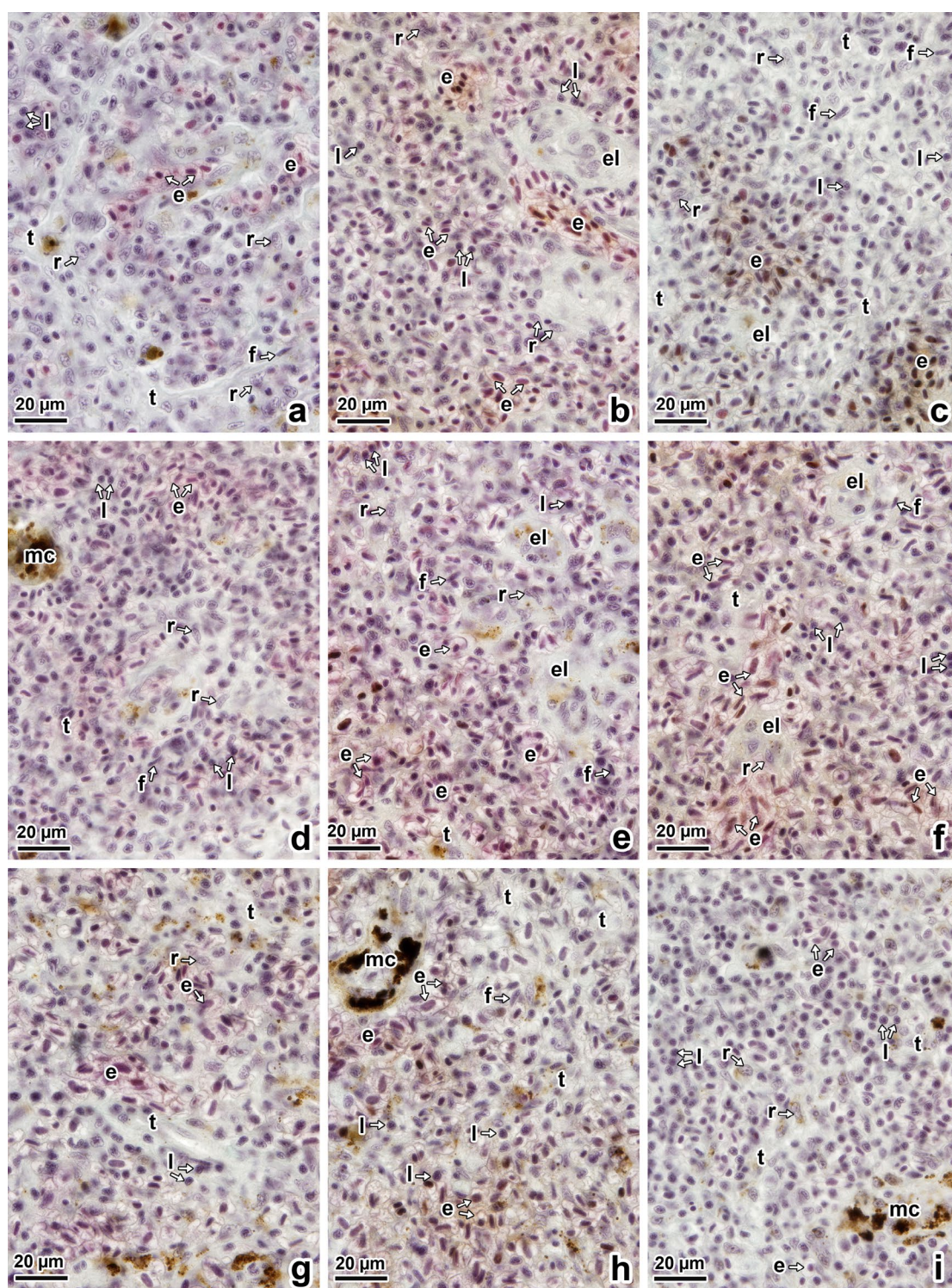


Fig. 9. High magnification of splenic parenchyma in all fish lines. (a) Pure *C. carpio*. Splenic parenchyma showing a well-developed trabecular network and indistinct ellipsoids. (b) Pure *C. gibelio*. Splenic parenchyma showing distinct ellipsoids and erythrocyte accumulations with a hint of rusty to brown discolouration. Note the clusters of enlarged erythrocytes. (c) F1 *C. gibelio* × *C. carpio*. Splenic parenchyma with abundant and thick trabeculae lacking regular organisation and indistinct ellipsoids. Note the clusters of enlarged erythrocytes and brown discolouration. (d) F1 *C. carpio* × *C. gibelio*. Splenic parenchyma showing few thin trabeculae and accumulated erythrocytes with a hint of rusty discolouration. (e) Backcross *C. gibelio* × F1 hybrid. Splenic parenchyma showing few thick but short trabeculae, distinct ellipsoids, and erythrocyte accumulations with rusty to brown discolouration. Note the scattered enlarged erythrocytes. (f) Backcross F1 hybrid × *C. gibelio*. Splenic parenchyma showing distinct ellipsoids and irregularly organised trabeculae. Note the erythrocyte accumulation with a hint of rusty to brown discolouration as well as scattered enlarged erythrocytes. (g) Backcross *C. carpio* × F1 hybrid. Splenic parenchyma showing few thick trabeculae and erythrocyte accumulation with a hint of rusty discolouration. Note the aggregates of considerably enlarged erythrocytes and scattered brown pigmentation. (h) Backcross F1 hybrid × *C. carpio*. Splenic parenchyma showing thin, irregularly organised trabeculae, accumulation of erythrocytes, and brown pigment deposits. Note the clusters of enlarged erythrocytes. (i) F2 generation. Splenic parenchyma showing medium-thick trabeculae and a small amount of scattered brown pigment. Applies to (a-i): paraffine sections stained with Masson's trichrome, BF-LM. e – erythrocyte; el – ellipsoid; f – fibroblast; l – lymphocyte; mc – melanomacrophage centres; r – reticular cell; t – trabeculae.